Progress in Nuclear Magnetic Resonance Spectroscopy 102–103 (2017) 15–31

Contents lists available at ScienceDirect

Progress in Nuclear Magnetic Resonance Spectroscopy

journal homepage: www.elsevier.com/locate/pnmrs

Monitoring protein folding through high pressure NMR spectroscopy

Julien Roche [a], Catherine A. Royer [b], Christian Roumestand [c,*]

[a] Roy J. Carver Department of Biochemistry, Biophysics and Molecular Biology, Iowa State University, Ames, IA 50011, USA
[b] Department of Biological Sciences, Rensselaer Polytechnic Institute, Troy, NY 12180, USA
[c] Centre de Biochimie Structural INSERM U1054, CNRS UMMR 5058, Université de Montpellier, Montpellier 34090, France

Edited by David Neuhaus and David Gadian

ARTICLE INFO

Article history:
Received 20 March 2017
Accepted 31 May 2017
Available online 2 June 2017

ABSTRACT

High-pressure is a well-known perturbation method used to destabilize globular proteins. It is perfectly reversible, which is essential for a proper thermodynamic characterization of a protein equilibrium. In contrast to other perturbation methods such as heat or chemical denaturant that destabilize protein structures uniformly, pressure exerts local effects on regions or domains of a protein containing internal cavities. When combined with NMR spectroscopy, hydrostatic pressure offers the possibility to monitor at a residue level the structural transitions occurring upon unfolding and to determine the kinetic properties of the process. High-pressure NMR experiments can now be routinely performed, owing to the recent development of commercially available high-pressure sample cells. This review summarizes recent advances and some future directions of high-pressure NMR techniques for the characterization at atomic resolution of the energy landscape of protein folding.

Contents

* Corresponding author.
E-mail address: christian.roumestand@cbs.cnrs.fr (C. Roumestand).

http://dx.doi.org/10.1016/j.pnmrs.2017.05.003
0079-6565/

1. Introduction

Since Anfinsen and colleagues [1] first studied the renaturation of reduced and unfolded ribonuclease A, much effort has been expended in attempting to understand the relationships between the amino acid sequence, the structure, and dynamic properties of the native conformation of proteins. Individual protein sequences have evolved to exhibit the level of stability, cooperativity and conformational dynamics required for their optimal function under the conditions in which the organism must survive: the native conformations of hundreds of proteins are known in great detail from structural determinations by X-ray crystallography and NMR spectroscopy. However, little is known about the conformations of denatured and partially folded states, which is a serious shortcoming in current studies of protein stability and protein folding pathways [2]. Since a general description of folding transition states and routes cannot be predicted for arbitrary amino acid sequences, protein folding energy landscapes remain to be mapped experimentally. Likewise, a protein's propensity to aggregate cannot be deduced from its sequence. Finally, we do not know how sequence encodes the conformational fluctuations and heterogeneity required for function in specific contexts.

Characterization of all the non-native species (unfolded states, transition states and partially folded intermediates) encountered by proteins that fold in a barrier-limited manner is essential if we are to realize our quest to understand how proteins fold in all-atom detail. Substantial advances toward this goal have been realized for a handful of small proteins [3–9]. This has been enabled by the development of experimental approaches with faster timescales of measurement [10] and enhanced sensitivity [11], together with improvements in computing power and new theoretical tools [12–14]. Indeed, in recent years, improvements in experimental techniques and enhancements in computing power have revolutionized our understanding of the mechanisms of protein folding. Today, the arsenal of biophysical methods available to the experimentalist allows monitoring conformational transitions from picosecond to second (or longer) timescales with populations as little as 0.5% [15]. By combining insights gained from theory, experiment and simulation we are moving toward an atomistic view of folding landscapes.

Due to recent methodological advances, NMR spectroscopy has emerged as a particularly powerful tool to obtain high-resolution structural information about protein folding events because an abundance of site-specific probes can be studied simultaneously in a single one- or multidimensional NMR spectrum. Experiments can be recorded as kinetic measurements that monitor the return to equilibrium after an initial perturbation. For example, very slow folding events can be monitored directly in real-time [16], and recently developed fast acquisition methods allow the recording of two-dimensional NMR experiments for real-time folding studies with a time resolution of a few seconds [17,18]. For folding events on the more common millisecond to second timescale, proton/deuterium amide hydrogen exchange NMR spectroscopy studies have proven particularly successful in identifying intermediates [19–21].

Gathering information *in vitro* on the folding events for a given protein using NMR spectroscopy, or any other appropriate methods, needs the choice of an appropriate perturbation aimed at destabilizing its folded state. Several methods are possible to unfold a protein: adding chaotropic reagents (urea, guanidinium chloride), or modifying the physicochemical parameters of the sample (pressure, temperature, pH). One century ago, the coagulation of egg white by applying pressure of 700 MPa showed for the first time that pressure can denature protein [22]. In spite of difficulties for implementation, pressure is a method of choice to unfold a protein: it is a "soft" method, generally reversible, that gives access to a large panel of thermodynamic parameters specific to the folding/unfolding reaction [23,24]. As noted later, the physical basis for the effects of pressure on protein structure and stability remains controversial, in contrast to a relatively clear physical understanding of temperature effects [25–27]. The fundamental observation of pressure effects has been that, over most of the accessible temperature range, the application of pressure leads to the unfolding of proteins, indicating that the volume change upon unfolding is negative (ΔVu), i.e., the specific molar volume of the unfolded state is smaller than that of the folded state (reviewed in [28]). As will be discussed later, the elimination of the solvent-excluded internal voids due to imperfect protein packing, rather than the differential hydration of individual atoms, likely represents the largest contribution to the magnitude of ΔVu [29–31]. Under the influence of high pressure, water molecules are believed to penetrate into internal cavities of the protein core and to induce the destabilization of hydrophobic interactions [30,31]. Because solvent-excluded cavities are not uniformly distributed but rather depend on the unique structural characteristics of a protein structure, the pressure-induced unfolding originates from specific, local and unique properties of the folded state. In this sense, it is very different from unfolding by temperature or chemical denaturants, which act globally and depend on exposed surface area in the unfolded state. Thus, the combination of high pressure and NMR constitutes a powerful tool that can lead to new knowledge about the role of residue packing in protein stability and of conformational fluctuations in water penetration, or that can be used to describe folding intermediates or other details of the energy landscape, otherwise invisible when using other approaches.

In the following, after a brief mathematical description of the pressure-temperature diagram of protein unfolding and of the origin of the parameter ΔVu (the volume difference between the unfolded and the folded state) that controls protein unfolding under pressure, we will discuss the use of NMR spectroscopy to monitor the unfolding reaction and to analyze the multiplicity of states that are sampled during this process, characterizing the "energy landscape" associated with protein unfolding [32–33]. A few lines will be dedicated also to describing how the technical difficulties involved in carrying out NMR at high pressure have been overcome.

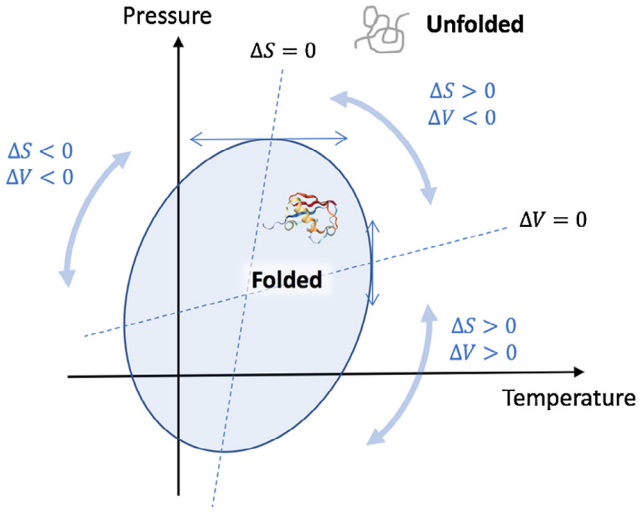

Fig. 1. Schematic representation of the elliptic p-T phase diagram as described by the Hawley formalism. The boundary of the phase diagram corresponds to conditions where $\Delta G = 0$. The slopes of the tangent to the ellipse define the sign of the first order derivatives, ΔS and ΔV. Adapted with permission from [37].

2. The pressure-temperature phase diagram of protein unfolding

2.1. Mathematical description

The so-called pressure-temperature (p-T) phase diagram is a phenomenological framework that explains the heat, cold and pressure denaturation of proteins in a unified picture. The general thermodynamic description of the elliptic phase diagram was first developed by Hawley in 1971 [34], by analyzing the pressure and temperature denaturation data measured on chymotrypsinogen [34] and ribonuclease A [35] under similar stability conditions ($\Delta G_U^0 \sim 2.5$ kcal/mol at pH ~ 2).

Assuming a two-state folding reaction, the derivative of the free-energy difference between the unfolded and folded states, $\Delta G_u = G_{unfolded} - G_{folded}$, with respect to temperature and pressure: $d\Delta G_u = \Delta V_u dp - \Delta S_u dT$, is integrated through a second order Taylor series expansion around the pressure and temperature reference points p_0 and T_0:

$$\Delta G_u(p,T) = \Delta G_u^0 - \Delta S_u^0(T-T_0) + \Delta V_u^0(p-p_0) + \frac{\Delta\beta_u}{2}(p-p_0)^2 + \Delta\alpha_u(p-p_0)(T-T_0) - \Delta C_p\left[T\left(\ln\frac{T}{T_0}-1\right)+T_0\right] \quad (1)$$

where the first order derivatives ΔS_u and ΔV_u correspond to the change of entropy and volume upon unfolding respectively. The second order derivatives, namely the change of compressibility ($\Delta\beta_u$), expansivity ($\Delta\alpha_u$) and heat capacity (ΔC_p) are defined as:

$$\Delta\beta_u = -\frac{1}{V}\left(\frac{\partial\Delta V_u}{\partial p}\right)_T; \quad \Delta\alpha_u = \left(\frac{\partial V_u}{\partial T}\right)_p; \quad \Delta C_p = T\left(\frac{\partial\Delta S_u}{\partial T}\right)_p \quad (2)$$

The Hawley equation corresponds to the general equation of a conic and could theoretically match with either an ellipse, a parabola or a hyperbola [36]. The condition for an elliptic shape is given by: $\Delta\alpha_u^2 > \frac{\Delta C_p \Delta\beta_u}{T_0}$, which has been verified so far in all protein study cases, typically because of the opposite signs of ΔC_p and $\Delta\beta_u$ (i.e. $\Delta C_p > 0$ and $\Delta\beta_u < 0$) [37]. The slope of the tangent to the ellipse: $\frac{\partial p}{\partial T} = -\left(\frac{\partial\Delta G_u}{\partial T}\right)/\left(\frac{\partial\Delta G_u}{\partial p}\right)$ is equal to 0 for $\Delta S = 0$ and infinity for $\Delta V = 0$ (Fig. 1) [38]. The first order derivatives, ΔS and ΔV, control the position of the ellipse center in the p-T plane whereas the second order derivatives determine the global shape and orientation of the phase diagram. A decrease of ΔC_p or $\Delta\beta$ broadens the ellipse in the direction of the temperature or pressure axis respectively, while $\Delta\alpha$ controls the orientation of the ellipse [39].

2.2. Limitations of the p-T phase diagram

The elliptic shape of the p-T phase diagram arises from the second order truncation of the Taylor series, which implies that the second order derivatives, $\Delta\beta_u$, $\Delta\alpha_u$ and ΔC_p, are assumed not to change with temperature or pressure. While this has been a reasonable assumption for all of the protein systems studied so far, it should be noted that, in principle, all three second-order derivatives can potentially be pressure- or temperature-dependent. Indeed, Yamaguchi et al. noticed a small pressure dependence of the difference in heat capacity, ΔC_p, for ribonuclease A [40]. Nevertheless, Smeller pointed out that third order terms can be included in the Hawley formalism without causing a major alteration of the elliptic shape of the p-T phase diagram [37].

It is also very important to notice that the elliptic model is based on the assumption of a two-state folding mechanism, which implies the absence of any folding intermediate state or molten globule. It also implies that the denaturated states populated in different regions of the phase diagram are all identical. However, several studies have shown that the pressure-, cold- and heat-denaturated states have distinct structural properties [41]. This observation was reported by Meersman et al. who analyzed the residual secondary structures of the denaturated states of myoglobin by FTIR spectroscopy in various pressure and temperature conditions [42]. Infrared spectroscopy was also used to compare the pressure- and heat-denaturated states of interferon-γ [43]. Based on NMR experiments, Griko and Kutyshenko found that the network of residual interactions in β-lactoglobulin is more extensive in the cold denatured states than in the heat-induced unfolded states [44]. The different denaturated states of staphylococcal nuclease have also been extensively studied using a combination of SAXS and FTIR experiments [45,46]. The general consensus emerging from these studies is that cold- and pressure-denaturated states of proteins are compact and more likely to contain residual secondary structures, while the heat-denatured states are closer to ideal disordered polymers.

Finally, it should be noted that the Hawley formalism describes the phase boundaries of protein stability in the context of a thermodynamic equilibrium. This implies that a reversible unfolding and folding reaction can take place in all the pressure and temperature conditions considered. However, it well known that heat denaturation can lead to the irreversible aggregation of globular proteins [43,47]. These aggregated states can potentially be treated as a distinct phase in the p-T phase diagram [48] and provide important information in the context of amyloid fiber formation [42].

2.3. Experimental determination of p-T phase diagrams

The complete determination of a p-T phase diagram requires measurement of the stability of a protein over a wide range of conditions, from low to high pressure and from cold to high temperature. Several experimental techniques have been employed over the past years to achieve this goal, including fluorescence, NMR and FTIR spectroscopy as well as small X-ray scattering and calorimetry techniques [41] (Fig. 2). Early on, Jonas and Akasaka's group managed to describe the phase diagram of ribonuclease A [49] and staphylococcal nuclease [50], using only NMR spectroscopy. They obtained the unfolding curves in various pressure and temperature conditions by monitoring the signals of histidine residues and extracted the first and second order thermodynamic parameters through a global fit of the data [49,50].

The very high pressure range accessible to infrared spectroscopy has also proven to be extremely useful for the characterization of p-T phase diagrams, either as a sole technique [51] or in combination with fluorescence spectroscopy [52]. Fluorescence has been used in the case of cytochrome c [53], lipocalin FluA [54] and hen lysozyme, in combination with NMR spectroscopy [55]. Among these globular proteins, the staphylococcal nuclease stands out as a model that has been extensively studied using a wide range of experimental techniques, including NMR, fluorescence, FTIR and SAXS [56] but also DSC, PPC and densitometry [38], allowing a very precise characterization of its p-T phase diagram.

3. The origin of ΔV of unfolding

It has been generally found that the volume change upon protein unfolding is negative, that is, the molar volume of the unfolded state is lower than that of the folded state [28]. The origins for this observation were hotly contested for many years. It has been suggested that the decrease in volume resulted from pressure-dependent modification of the properties of water [57]. However, it has been generally observed that the volume change of unfolding

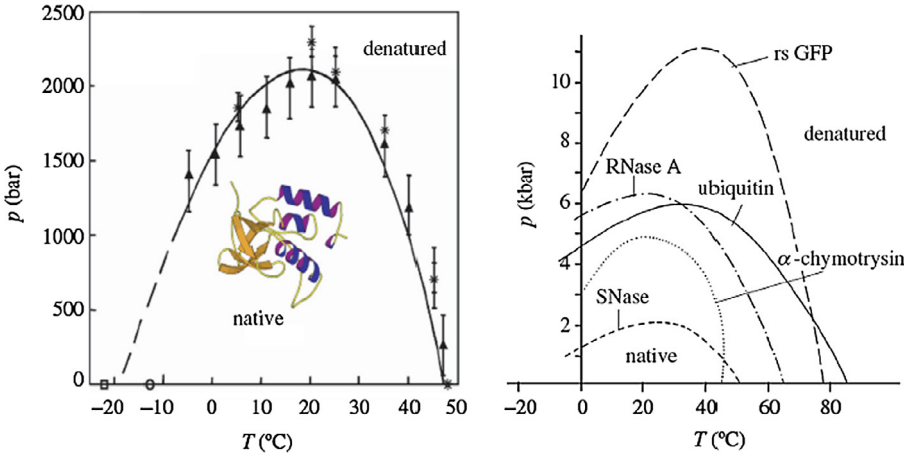

Fig. 2. Left: p-T phase diagram of staphylococcal nuclease determined from a combination of SAXS, FT-IR and DSC experiments at pH 5.5. Right: Overlay of the elliptic phase diagrams obtained for several globular proteins. Adapted with permission from [41].

is pressure-independent. This has two ramifications. The first is that the second order term (the differential compressibility between folded and unfolded states) does not significantly contribute to pressure-induced unfolding. The second is that the volume change cannot result from a pressure-induced modification of solvent properties, as this would by definition be pressure-dependent, contrary to observation.

Another possibility that has been suggested for the basis of the volume change of unfolding is that the density of water molecules around the protein surface is higher on average than in the bulk. Thus upon unfolding, and the exposure of more surface area, the increased number of water molecules interacting with this surface would lead to a decrease in volume. Pressure perturbation calorimetric studies on model compounds reveals opposite, and thus compensatory, densitometric behavior of polar and non-polar amino acids, as well a strong temperature dependence [58,59]. Experimentally Rouget et al. did not find any correlation between the size of a protein and the value of the volume change of unfolding [30]. In addition, it has been proposed, based on theoretical considerations of model compound transfer from the gas phase, that the contribution of hydrophobic hydration of exposed surface should actually increase (rather than decrease) the molar volume, consistent with the results from PPC on the model systems [60].

Finally, since the early days of pressure denaturation, it has been generally accepted that packing defects inside folded protein structures would contribute to a decrease in volume as they are largely eliminated upon unfolding [61–63]. Of course this is only true to the extent that these internal void volumes are solvent-excluded in the first place. Experimentally it has been shown that increasing the void volume by mutations that replace large hydrophobic amino acids results in the creation of internal cavities as verified by crystallographic studies [64,65]. The volume change for unfolding these cavity-containing variants is larger in absolute value than for their wild type counterparts. Some time ago, a pressure effect on hydrophobic interactions was proposed based on molecular dynamics simulations [66]. However, this theoretical result does not appear to be in contradiction with the idea that the volume change of unfolding is mainly geometric in origin. The major contribution to the volume change of unfolding appears to be solvent-excluded void volume in folded protein structures, which is eliminated upon unfolding. Of note, it has been shown using variants of staphylococcal nuclease harboring ionizable residues in their hydrophobic core, that the volume change of unfolding is consistently about 25 ml/mol larger in absolute value for these variants compared to what one would expect given the size of the amino acid substitution [67,68]. This argues for a contribution to the value of the volume change of unfolding from solvent density, through electrostriction of the exposed charge residues.

Concerning the effect of temperature on protein unfolding volume changes, which is quite strong, it should be stressed that the volume change is generally large and negative at low temperature and becomes smaller in absolute value, and even becomes positive in some cases, as temperature increases. This is due to the larger thermal expansion of the unfolded states of proteins compared to their folded states. The expansion of the unfolded state, which decreases mildly with temperature, is largely due to hydration effects [58,69]. That of the folded state includes hydration of the surface, but also expansion of the folded structure itself, which is limited by the interactions in the folded state [70,71]. The expansion of the folded state is strongly temperature dependent, decreasing much more than that of the unfolded state as temperature increases, due to constraints against expansion inherent in the folded structure.

In high-pressure NMR experiments, one measures signal changes from numerous (~50–150 for medium-sized proteins) individual residue resonances, usually pressure-dependent changes in the folded (or unfolded, when they are assigned) peak intensities in an HSQC spectrum. Care must be taken in interpreting the apparent values of ΔV_u and ΔG_u obtained from fitting each of these intensity vs pressure profiles. Indeed, these spectroscopically derived values (or any other observable) only truly correspond to these thermodynamic parameters if the system conforms to a two-state model. In fact, we have found that this is very often not the case in pressure-induced unfolding. When a folding/unfolding equilibrium deviates from two state behavior, the width of the distribution of the recovered residue-specific apparent ΔV_u and ΔG_u values is merely a reflection of the complexity of the folding/unfolding transition.

Finally, one has to keep in mind that the experimental measurement of ΔV yields the volume change of *all the system* under study: not only the volume of unfolding of the protein, but also the ΔV of the buffer. In general, anionic buffers, such as phosphate and dimethyl-glutarate (DMG), have negative and relatively high ΔV values, although cationic and zwitterionic buffering agents (ACES, HEPES, MES, Tris, ...), described by Good et al. [72], have positive and relatively low ΔV values. Thus, measuring the ΔV of unfolding of a protein dissolved in an anionic buffer would inevitably give an erroneous value for this parameter. In addition, the pH of an anionic buffer is strongly dependent on pressure. Indeed, water molecules pack more closely around free ions, a phenomenon known

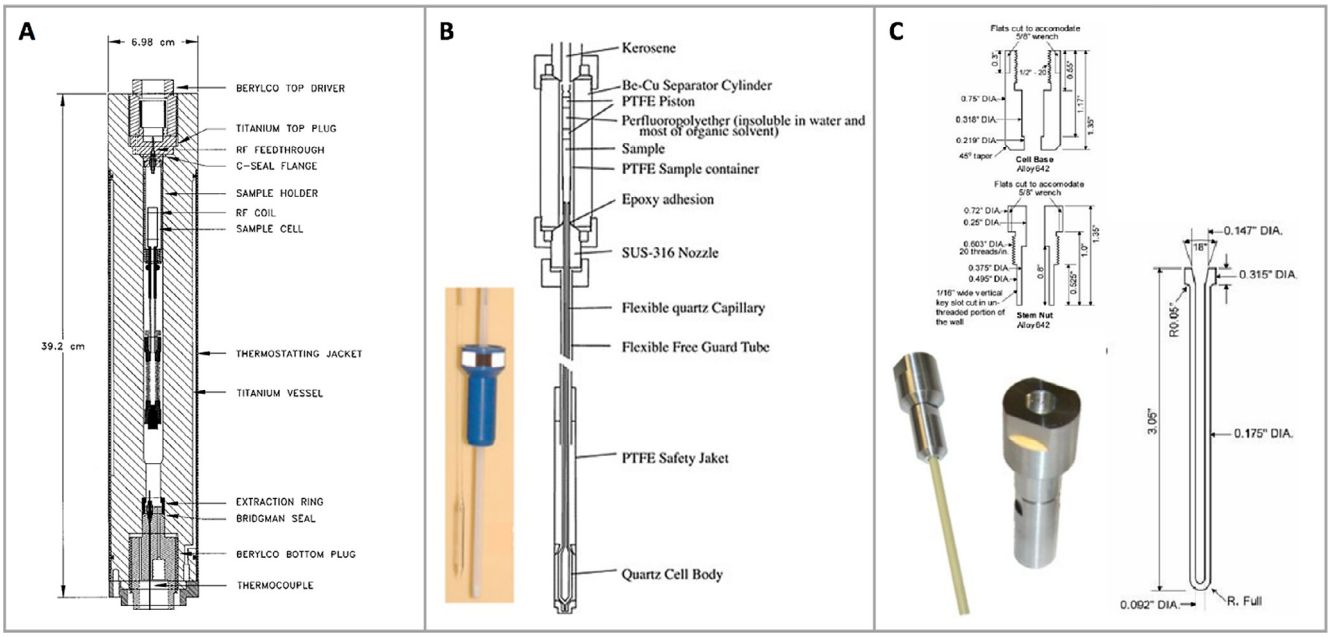

Fig. 3. Three different designs of high-pressure NMR instrumentation, from the original "autoclave" method to the modern high-pressure sample cells. A: Schematic representation of the titanium high-pressure vessel designed by Jonas and coworkers for a 300 MHz spectrometer (adapted from [84]). B: On-line cell design developed by Yamada et al. [88], with a picture of the quartz cell together with a protecting tube made of Teflon (adapted from [91]). C: Design of the high-pressure tube developed by Peterson et al. [95] made from aluminum-toughened zirconia, together with its non-magnetic connection base. The picture showing the assembled tube is reproduced with permission from http://www.daedalusinnovations.com (Daedalus Innovation™).

as electrostriction, resulting in a net reduction in volume of the system. According to the principle of Le Chatelier, the equilibrium will shift to minimize the effect of pressure, thus favoring the ionization of weak acids in water and resulting in large decrease in pH under pressure. The pressure dependence of pH has been determined for a large number of weak acids and bases [73–79]. Thus, the popular NMR phosphate buffer undergoes a decrease of about 0.4 pH unit for every 100 MPa increase in pressure, and for this reason many authors have raised concerns about its use in biological studies [80–82]. On the other hand, cationic buffers can be considered pH pressure insensitive [75].

4. High pressure NMR instrumentation

The first design for high-pressure NMR spectroscopy was originally developed by Benedek & Purcell in 1954 for the study of water and organic solvents under pressure [83]. With this setup, later called the "autoclave" method, the entire radiofrequency transmitter and detection coils are placed in a high-pressure non-magnetic vessel (Fig. 3A). This method was then refined by Jonas and coworkers to be compatible with the higher magnetic fields required for the study of biomolecules [84–86]. The "autoclave" approach gives access to very high pressure (~9 kbar) but the incompatibility of this design with modern NMR probe electronics has limited its further application, especially for biological samples for which multidimensional and multinuclear experiments are critically needed.

An alternative approach, based on pressure-resistant sample cells, instead of pressure-resistant probes, emerged in the mid-70s and largely circumvented the limitations of the original "autoclave" design [87]. These high-pressure sample cells can be used with any commercial NMR probes and allowed the measurement of multidimensional and multinuclear experiments with very good field homogeneity. It consists of an external source of hydrostatic pressure (a hand oil-pump) connected by a long capillary to a quartz cell protected by a Teflon tube that goes into the detection coil (Fig. 3B) [88]. This approach has been popularized by Akasaka and coworkers who used the high-pressure cell method to characterize the folding mechanism of numerous globular proteins [89]. Despite its broad application, the design developed by Yamada et al. [88] suffers from certain limitations, mainly the delicate hand-made manufacturing of the quartz cell and the small sample volume available (about 40 μL) requiring highly concentrated protein samples [90,91].

In 1996 Wand and coworkers developed, as an alternative to the quartz cell method, a large volume NMR tube assuring a high signal to noise ratio and capable of kilobars of pressure using a novel method for joining a sapphire tube to a pressure manifold [92]. A complementary approach, also based on a sapphire tube, was later proposed by Arnold et al. [93] while ceramic was chosen by Erlach and coworkers for the design of a new high pressure tube with a safety valve [94]. The high-pressure sample cells currently commercially available are made from aluminum-toughened zirconia and mounted on a self-sealing non-magnetic valve (Daedalus Innovation™) [95] (Fig. 3C). These tubes are rated to pressures up to 300 MPa and can be used with any commercial NMR probe with a sensitivity of about 50% of a standard 3 mm diameter NMR tube. Mineral oil is generally used to transmit pressure and no physical separation is therefore needed between the protein sample dissolved in a water-based buffer and the transmitting fluid. It should be noted that the pressure range allowed by these pressure cells is significantly more limited (maximum 300 MPa) than the one authorized by the "autoclave" method (up to 900 MPa), and may be insufficient to readily unfold a protein in physiological conditions. Nevertheless, this drawback can be easily circumvented by playing with other physico-chemical parameters (temperature, pH...), or by adding sub-denaturing concentrations of chaotropic reagents (urea, guanidinium chloride (GuHCl)...) to the buffer, in order to decrease ΔG, thus allowing the protein to unfold in the pressure range authorized by the pressure cell.

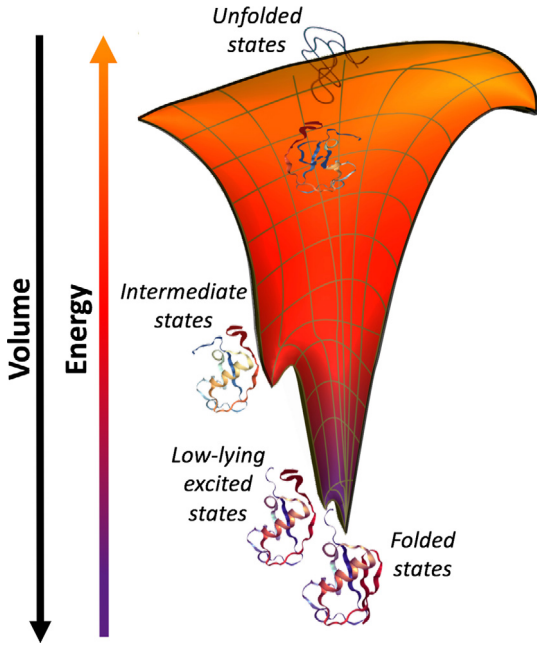

Fig. 4. Pictorial representation of the energy landscape describing protein folding. The ensemble of denatured conformations, including conformational ensembles at different stages of the folding process discussed further, is "funnelled" into the unique native structure. Illustrating the "protein volume theorem" [102,103], the higher energy conformational sub-states occupy a smaller molar volume than the lower energy conformers. Therefore, an increase in pressure tends to destabilize the native states and shifts the equilibrium toward the partially or completely unfolded states.

5. Exploring the energy landscape associated with protein folding using High-Pressure NMR

In combination with high pressure, NMR is a technique able to reveal unprecedented details of the folding and unfolding mechanisms of globular proteins at atomic resolution [31,96]. Steady-state measurements give access to thermodynamic parameters such as the free energy difference between the folded and unfolded states of the protein, or to more specific parameters such as ΔV_u that report on the cooperativity of the unfolding/folding reaction. Kinetic measurements give access to the unfolding/folding rates and to the characterization of transition states between unfolded and folded states (Transition State Ensemble volume). In this way, the entire distribution of the different states populating the energy landscape describing protein folding can be reached with atomic resolution, from the folded to the unfolded states (Fig. 4).

5.1. Detecting low lying conformational states with high-pressure NMR

Proteins are generally thought to fold into a "single" conformer that is thermodynamically most stable under physiological conditions, normally identified as the native structure [1]. Nevertheless, because of residual frustration of the free-energy landscape, many protein ground states are found in equilibrium with higher-energy conformational sub-states. They are commonly referred to as "low-lying" excited states because they lie within about 10 kJ/mol just above the lowest energy conformation at the bottom of the folding funnel [23,97–101]. These sub-states can rarely be directly detected under physiological conditions by spectroscopic techniques. This is largely because they are usually hidden within the overwhelming population of lowest-energy conformers. Since chemical shifts are very sensitive probes to the local structure of proteins, their analysis as a function of pressure may help to reveal the existence of such sub-states. Of course, this implies that these high-energy sub-states have a lower partial molar volume than the native state. This is stipulated by the "protein volume theorem" proposed by Akasaka and coworkers (Fig. 4): *the partial volume of a protein decreases in parallel with the decrease of the conformational order* [102,103].

Based on the analysis of the pressure dependence of ^{1}H chemical shifts for a set of 8 globular proteins, Akasaka and Li observed a general, non-specific, downfield shift of the ^{1}H chemical shifts [98]. The origin of the ^{1}H chemical shift changes induced by pressure has been studied extensively and shown to be strongly correlated with the change of the hydrogen-bond lengths [98,104,105]. Thus, the downfield shifts of amide ^{1}H are thought to originate from the compression of hydrogen bonds induced by pressure. This effect has been directly measured by Nisius and Grzesiek with through-hydrogen bond $^3J_{NC'}$ couplings, describing the pressure and temperature stability of the hydrogen bond network of ubiquitin [106]. Analysis of the effect of pressure was later extended to the $^1H_\alpha$ and ^{13}C chemical shifts by Wilton et al. on the protein G and barnase revealing that pressure induces a general upfield shift for these two nuclei [107,108]. For the ^{15}N and ^{13}C chemical shifts, the interpretation is more complex. Pressure-induced changes of the $^{13}C_\alpha$ shifts are thought to originate from slight compressions of covalent bonds [107,108]. ^{15}N chemical shifts, in theory, depend on hydrogen bonding both to amide nitrogen and amide carbonyl, as well as on backbone dihedral angles and side chain orientations [109].

Besides the linear shifts, the non-linear pressure response of the ^{1}H chemical shifts showed much more variability among the 8 proteins initially investigated by Akasaka et al., and was attributed to the presence of low lying conformational sub-states within the folded states basin [98]. Thus, pressure dependent changes of the chemical shift $\delta(p)$ can be fitted well by a second order Taylor expansion as:

$$\delta(p) = \delta_0(p_0) + B_1(p - p_0) + B_2(p - p_0)^2 \quad (3)$$

Here, $\delta_0(p_0)$ is the chemical shift at atmospheric pressure p0 of 0.1 MPa, and B_1 and B_2 the first (linear) and second order pressure coefficients [110]. Kalbitzer and coworkers reported recently a series of careful parameterizations of the linear and non-linear factors for the pressure dependence of the ^{1}H, ^{13}C, and ^{15}N chemical shifts using simple model peptides [111–113]. These first order and second order parameters measured on model peptides are particularly useful in order to distinguish real pressure-induced conformational changes on a globular protein from the non-specific effects of pressure on chemical shifts. In addition, Kalbitzer and coworkers also recently published a more in-depth interpretation of non-linear chemical shift changes based on protein structural fluctuations, showing that the ratio of the first- and second-order pressure coefficients B_1 and B_2 was related to the ratio of the compressibility $\Delta\beta'$ and partial molar volumes ΔV [114].

Further analysis of the effect of pressure on ^{1}H and ^{15}N chemical shifts of different proteins by Kitahara et al. reveals that residues around water-excluded cavities exhibit large deviations from the average values, indicating again that cavities can be an important source of conformational fluctuation in globular proteins [108]. An example of such structural fluctuations around internal cavities has been reported recently in a study of the human prion protein, showing a correlation between the xenon binding sites and the regions exhibiting non-linear chemical shift perturbation as a function of pressure [115]. It has also been demonstrated for several globular proteins that high-pressure was able to stabilize partially folded conformers prior to complete unfolding. The thermodynamic properties of such on-pathway molten globules

or intermediate states have been characterized for the Ras binding domain of RalGDS [116], rPrP prion protein [117], ubiquitin [102], sperm whale apomyoglobin [118] and outer surface protein OspA [119]. In the case of β-lactoglobulin [120] the free-energy difference between the native states and an excited conformer was found to be in good agreement with ΔGHX values measured from H/D exchange experiments [121], suggesting that the high-pressure stabilized conformers were similar to the "open" conformations sampled at atmospheric pressure.

Even if pressure can significantly stabilize conformational sub-states with a lower molar volume, a precise structural characterization of these non-native states represents a considerable challenge. Williamson and Akasaka first proposed a method to describe the structural changes occurring at high-pressure from the pressure dependence of the chemical shifts. This method was successfully applied to BPTI [122] and hen lysozyme [123], revealing a global shortening of H-bonds and large structural changes for residues close to buried water molecules. In 2005, Kitahara et al. reported the first ab initio structure determination of a high-pressure stabilized conformer for ubiquitin [100], which was later found to be similar to the structure of the mutant Q41N [124]. The structure of the high-pressure conformer is characterized by a partial opening of the protein core at the C-terminal side and a 5% increase of the surface area with respect to the native structure. Several MD simulation studies have later shown that this conformational change promotes the penetration of water molecules in the protein core [124–126].

5.2. Folding cooperativity and folding intermediate states

Most globular proteins are known to deviate from a true two-state folding mechanism and ideal global cooperativity by populating en route intermediate folding states. This is what leads to the concept of "foldons" [21,127], which are local regions that fold with different characteristics than other regions of the protein. Such partially unfolded intermediates can be characterized using NMR spectroscopy that allows a residue-specific analysis of the folding process. Indeed, the atomic resolution offered by NMR experiments provides an intrinsic multi-probe approach to assess the degree of protein folding cooperativity, which is otherwise difficult to characterize using techniques such as circular dichroism or fluorescence. In addition, the high reversibility of pressure unfolding/refolding experiments ensures a proper thermodynamic characterization of the process, which is often problematic to assess by heat denaturation because of excessive aggregation. Amide protons offer ideal probes to monitor the unfolding reaction: each amino acid bears a HN group, with the exception of proline which is generally a minority residue in the composition of soluble proteins (<3%), and the corresponding proton resonances represent the most resolved region of the proton spectrum of a protein. This resolution can be considerably enhanced with the use of 2D NMR spectroscopy, through homonuclear (COSY, TOCSY, NOESY) or, better, heteronuclear ([^{1}H-^{15}N]-HSQC) experiments. In addition, their acidic character makes them well suited for proton/deuteron exchange measurements, a property that has been extensively used to evaluate the local stability of a protein, sometimes in combination with high pressure, as it will be discussed further.

5.2.1. High-pressure and protein folding cooperativity: steady-state measurements

The pressure-induced unfolding reaction, which occurs on a slow NMR time-scale, is usually analyzed by monitoring the decrease in cross-peak volume or intensity for cross-peaks of the native state in a series of ^{1}H-^{15}N experiments recorded at increasing pressure (Fig. 5). Care must be taken that these measurements be recorded when the equilibrium between native population/unfolded population has been reached after a pressure jump. This equilibrium needs a variable period of time (the relaxation time) ranging from several hours to a few minutes or often much less [64]. This type of experiment can be analyzed by individually fitting the intensity profile of each residue as function of pressure, yielding residue-specific apparent ΔV_u values [64,128].

The fact that the observed intensity profile measured for each residue is usually sigmoidal makes reasonable the assumption of a two-state equilibrium between the native (N) and the denatured (D) state of a protein at the residue level. Thus, the equilibrium constant K_{eq} between N and D may change with pressure according to the relation:

$$K_{eq} = [D]/[N] = \exp(-\Delta G/RT) \tag{4}$$

where

$$\Delta G = G_D - G_N = \Delta G^0 + \Delta V^0(p - p_0) - 1/2\Delta\beta V^0(p - p_0)^2 \tag{5}$$

Here ΔG and ΔG_0 are the Gibbs-free energy changes from N to D at pressure p and p0 (=0.1 MPa), respectively; ΔV^0 is the partial molar volume change; $\Delta\beta$ (=$-1/V^0/x\ \delta V/\delta p$) is the change in compressibility coefficient, R is the gas constant, and T is the absolute temperature. If we assume a negligible compressibility in the pressure range used to unfold the protein, the expression of ΔG simplifies to:

$$\Delta G = \Delta G^0 + \Delta V^0(p - p_0) \tag{6}$$

Using NMR spectroscopy, the observable will be I, the intensity (or volume) of the amide cross-peak corresponding to a given residue in the HSQC spectrum of either the folded species or of the unfolded species. Note that, usually, the spectrum of the folded species is considered because (i) it is usually fully assigned at this step, which is rarely the case for the spectrum of the unfolded species, and (ii) the spectral resolution is much better than in the spectrum of the unfolded protein where a lot of cross-peaks overlap, especially in the ^{1}H dimension. Thus, the equilibrium constant can be written as:

$$K_{eq} = \frac{[D]}{[N]} = \frac{I_N - I}{I - I_D} \tag{7}$$

where for a given residue, I_N stands for the intensity of the corresponding amide cross-peak in the native spectrum at 1 bar ($I_N = I_{max}$), while I_D corresponds to the intensity of the *same* cross-peak at high pressure, when the protein is fully unfolded ($I_D = I_{min}$). Combining this equation with Eq. (6) gives:

$$I = \frac{I_N + I_D e^{-[\Delta G^0 + (p-p0)\Delta V^0]/RT}}{1 + e^{-[\Delta G^0 + (p-p0)\Delta V^0]/RT}} \tag{8}$$

the characteristic equation for a two-state equilibrium. Contrary to fluorescence spectroscopy or circular dichroism, for instance, which gives a "global" value for the parameters ΔG^0 and ΔV^0, NMR yields "local" residue specific values of ΔG^0 and ΔV^0. Large variations in the ΔV^0 values measured for different residues of a given protein typically reflect departure from an ideal cooperative unfolding transition and inform on the potential presence of intermediate states [64,129]. This was reported for the protein Δ+PHS Staphylococcal Nuclease (SNase) [64]: if most of the residues report a similar ΔV^0 of ≈80 ml/mole, a value close to the "global" value measured with fluorescence spectroscopy, in some areas of the protein the measured residue-specific ΔV^0 values fall below this average value (<30 ml/mole) (Fig. 6). In terms of ΔG^0, it means that some regions of the protein are less stable than others, or that some regions of the protein unfold before others, suggesting the presence of folding intermediates, i.e. partially folded conformers having some degree of stability, in the protein energy landscape.

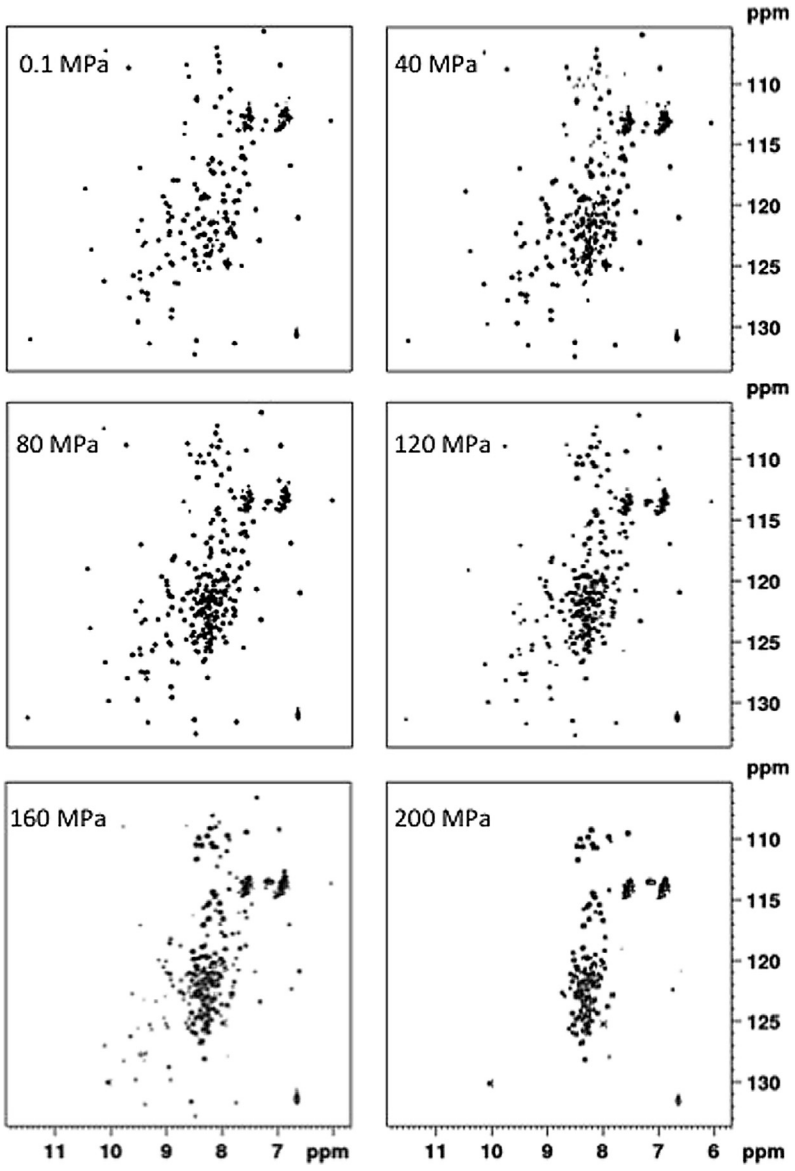

Fig. 5. Pressure dependence of the [^{1}H-^{15}N] HSQC spectrum recorded at 600 MHz on Δ+PHS Staphylococcal Nuclease at 298 K, pH 7 (Tris 10 mM) and in the presence of 1.8 M of guanidinium chloride. The Daedalus Innovation™ system described above was used to pressurize the sample.

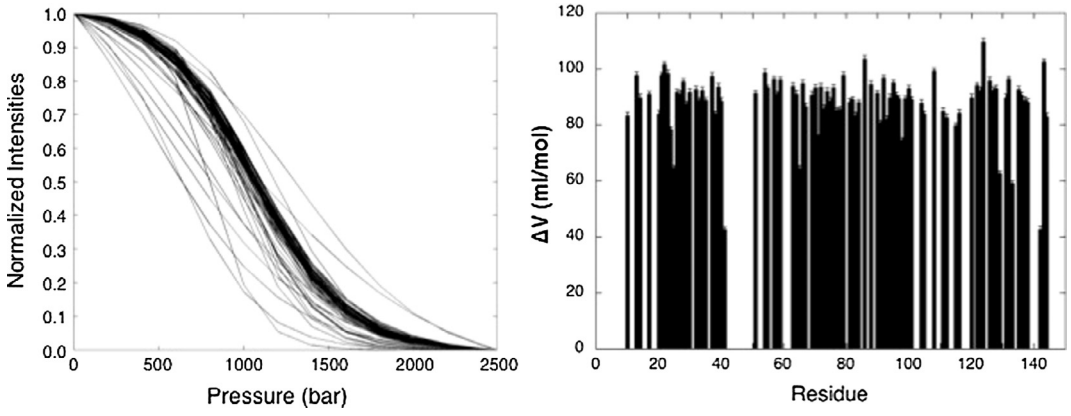

Fig. 6. Site-Specific monitoring of Δ+PHS SNase unfolding. Left: overlay of the normalized residue-specific denaturation curves obtained by fitting the decrease of the intensity of the corresponding cross-peaks measured in the 2D [^{1}H-^{15}N] HSQC spectra recorded at variable pressure (See Fig. 5). Right: ΔV values obtained through the fit of the intensity decrease of the 2D [^{1}H-^{15}N] HSQC cross-peaks with pressure, plotted versus the protein sequence (from results reported in [64]).

A problem often faced when monitoring such intensity profiles is that the observation is typically limited to the cross-peaks of the folded state. Whether the loss of intensity is due to local unfolding or to the presence of a high-energy sub-state with a distinct structure remains in most cases undetermined. This has led to a recent controversy on the nature of the pressure-induced unfolding pathway of T4 lysozyme [130,131]. When it is possible, a way to address such problem of interpretation is to compare for each residue the intensity profiles of the folded and unfolded cross peak, as recently demonstrated for the mature HIV-1 Protease [129]. However, the complete assignment of the pressure-denaturated state is often very challenging, as quoted before.

Residue-specific unfolding data can also be analyzed in terms of fractional contact map, defined as the product, or better the geometric mean [132], of the normalized intensities measured at a given pressure for the amide resonances of the two residues forming a native contact [31,64,133]. This approach was inspired by the analysis method used by Munoz and coworkers to characterize the thermal unfolding of the downhill protein BBL [134,135]. After normalizing the residue-specific denaturation curves obtained from the amide cross-peak intensity decays measured on the HSQC experiments recorded at variable pressure, the value of 1 for a given cross-peak ($I = I_N = 1$) can be associated with a probability of 1 (100%) for the corresponding residue to be in a native state, with all the native contacts present. Similarly, a residue for which, at the same pressure, the corresponding cross-peak has disappeared ($I = I_D = 0$) from the HSQC spectrum has a probability equal to zero to be in a native state: it belongs to an unfolded state where all the native contacts are lost. Now, consider two residues i and j in an intermediate situation where the probabilities to be in a folded state are p(i) and p(j), respectively, at a given pressure. If these two residues are close together in the native state, the probability p(i,j) to be still in contact at the same pressure is given by the geometric mean of the individual probabilities $p(i,j) = [p(i) \times p(j)]^{1/2}$. A contact map can be easily built from the 3D crystal or NMR structure of the protein by measuring all contacts between different atoms: usually, only the distances between Cα atoms of the different residues are used, and a "contact" between two residues i and j is defined by a distance Cαi- Cαj ≤ 8 Å. These contacts are then plotted in a diagonal diagram with the protein sequence numbering on the X and Y axes. Using a color code (for example) to report the probability of contact in this diagonal map, this gives a pictorial representation of the contacts lost in the protein at a given pressure (Fig. 7).

Fractional contact maps determined from pressure unfolding experiments can also be combined with Go-model molecular-dynamics simulations to obtain a structural representation of the conformational ensemble populated at high pressure [64]. If it is easy to calculate a contact map from a known 3D structure, it is also possible to calculate a 3D structure from a contact map, using the contacts as restraints in molecular dynamics simulations. Restraint lists can be obtained from a contact map and used for molecular modeling, with the possibility to "weight" the restraints with contact probabilities calculated at a given pressure. In this way, a large number of restraint lists will be generated, instead of one. For example, a contact between two residues associated with a probability of 0.8 will be randomly added to 80 lists out of 100, if the probability is only 0.4, the corresponding restraints will be in 40 lists out of 100, etc... One independent MD simulation is then run for each restraint list and the conformations generated by all the simulations analyzed collectively. In the case of the protein Δ+PHS SNase, such an analysis allowed us to identify a population of conformers corresponding to a folding intermediate where the C-terminal α-helix is unfolded whereas the N-terminal ß-barrel maintains its native structure (Fig. 8).

5.2.2. High-pressure and protein folding cooperativity: H/D exchange measurements

The early steps of unfolding can also be detected using H/D exchange measurements, a well-established NMR technique developed by Englander and coworkers [136] and designed to identify subunits with distinct local stabilities in globular proteins. In such experiments, protonated samples are typically lyophilized and then quickly dissolved in D_2O buffer just prior to measurements. Series of HSQC spectra are then recorded and the decrease of individual cross-peak intensities is monitored over time, reflecting the exchange of amide protons with the deuterated buffer. The Hydrogen ↔ Deuterium exchange reaction is classically described as a two-step reaction characterizing a transient structural opening reaction of the protein that exposes an amide proton to the solvent:

$$Close(H) \underset{k_{cl}}{\overset{k_{op}}{\leftrightarrow}} Open(H) \overset{k_{rc}}{\leftrightarrow} Open(D)$$

The steady-state exchange rate is given by:

$$k_{ex} = \frac{k_{op}k_{rc}}{k_{op} + k_{cl} + k_{rc}} \quad (9)$$

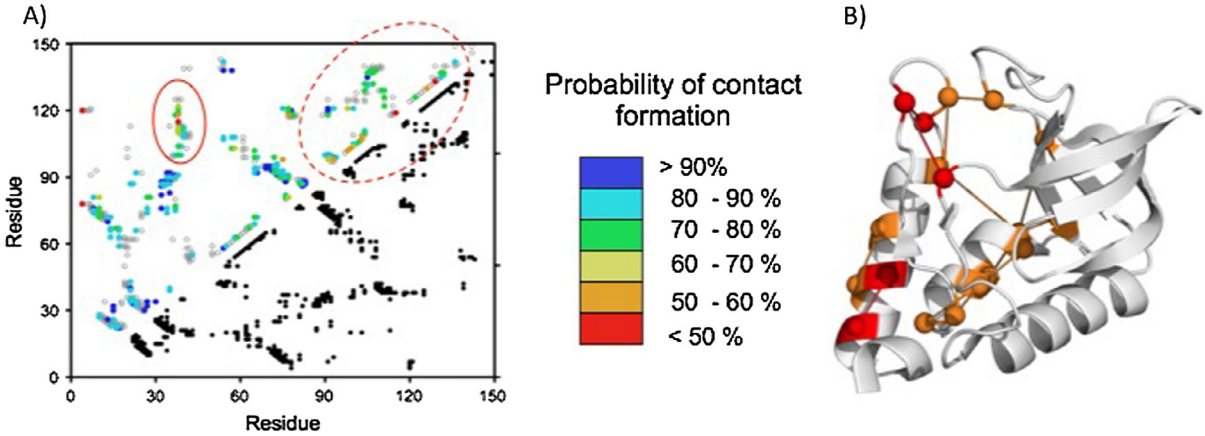

Fig. 7. Tracking Folding Intermediates with High-Pressure. (A) Fractional contact map built from the crystal structure of Δ+PHS SNase. The contacts above the diagonal have been colored with the code used for the probability of contact formation calculated at 80 MPa. The two ellipses show the zones where contacts are weakened at this pressure. (B) Ribbon structure of Δ+PHS SNase where Cα-Cα contacts weakened at 80 MPa are displayed in red (probability of contact <50%) and orange (50% < probability of contact <60%) (from results discussed in [64]).

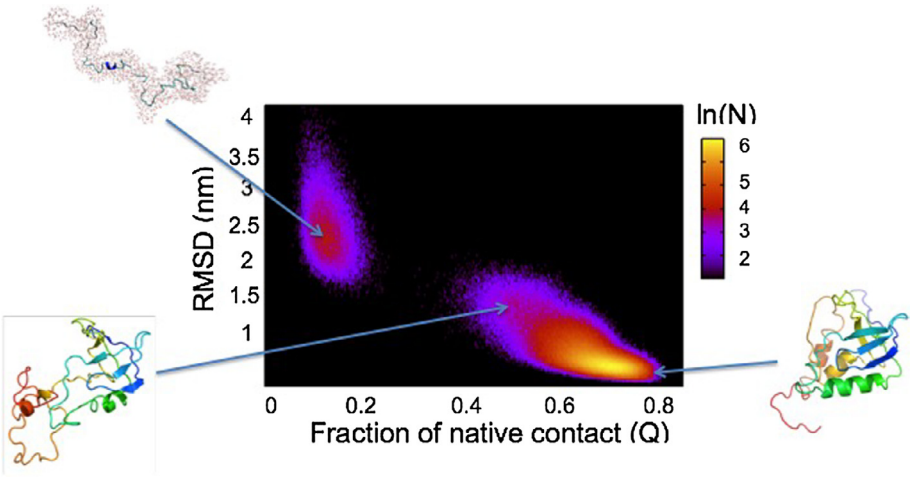

Fig. 8. Pseudo free-energy map calculated from Go-model simulations, based on the probability of contacts calculated at 80 MPa from residue-specific denaturation curves of Δ+PHS SNase in 1.8 M GuHCl. The root-mean-square-deviation calculated after clusterization of the 400,000 conformers obtained from these simulations is plotted as a function of the fraction of native contact. The color code represents the relative population of the different clusters. The structural cartoons show representative conformers of the native structure (RMSD ≈0.2 nm and Fraction of native contact ≈0.8), of an intermediate state (RMSD ≈ 1.3 nm and Fraction of native contact ≈ 0.5), and of a conformer representative of the unfolded state (RMSD ≈ 2.5 nm and Fraction of native contact ≈ 0.1) (from results discussed in [64]).

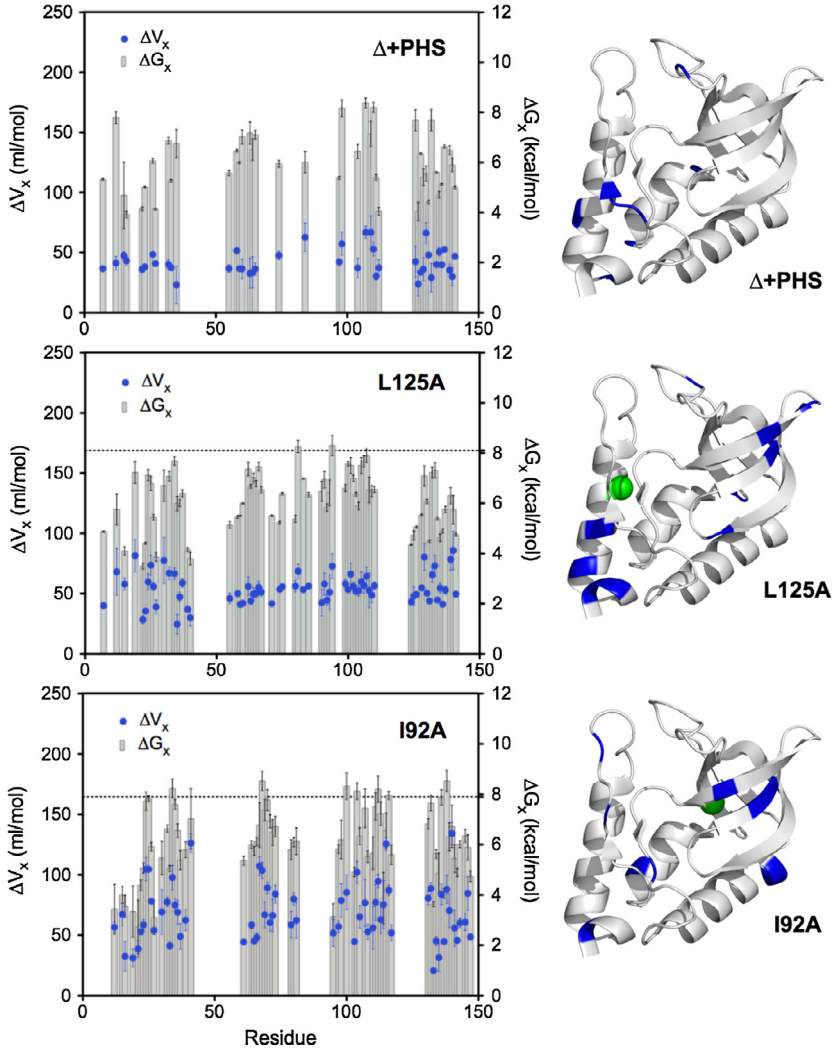

Fig. 9. High-pressure H/D exchange results obtained for the SNase pseudo-wt Δ+PHS and the cavity mutant L125A and I92A. *Left panel*: ΔV_x (blue points) and ΔG_x values (gray bars) are shown as a function of the protein sequence for all three proteins. *Right panel*: Residues with the largest ΔV_x values (more than 1 standard deviation) are indicated in blue on the protein structure, while the location of the mutated site is shown in green (adapted with permission from [31]).

where the rate of exchange, k_{ex}, is calculated from the rate of the opening and closing reactions, k_{op} and k_{cl} respectively and the rate of exchange for a fully exposed amide proton, k_{rc}. Most commonly, exchange in proteins below pH 9 occurs through the so-called EX2-limit where $k_{cl} \gg k_{rc}$ and the H/D exchange rate is defined as:

$$k_{ex} = \frac{k_{op}}{k_{cl}} k_{rc} = K_{op} k_{rc} \quad (10)$$

Under such conditions, the value of the constant K_{op} gives access to the free-energy for the underlying structural opening reaction:

$$\Delta G_x = -RT \ln K_{op} \quad \text{and} \quad \mathrm{PF} = \frac{1}{K_{op}} = \frac{k_{rc}}{k_{ex}} \quad (11)$$

Residues with large Protection Factors (PF) are usually located in the most stable regions of the protein, typically the hydrophobic core or a protected binding interface, while small PFs are usually measured for residues in the least stable or more dynamic regions of the protein. The rates of exchange of fully solvent-exposed amide protons (k_{rc}) are determined for each amino acid on the basis of model peptide studies and depend on the neighboring residues types, the pH of the buffer and temperature at which the experiment is recorded [137].

Fuentes and Wand were the first to combine H/D exchange experiments with pressure perturbation to examine the energetics of the apocytochrome b562, introducing for this purpose an additional correction to account for the effect of pressure on k_{rc} [138]. With increasing pressure, they observed a systematic increase in the rate of exchange, or, equivalently, a decrease in the calculated protection factors. Apparent volume changes for exchange (ΔV_x) were estimated from the linear dependence of the free energy of exchange with pressure ($\Delta G_x(p) = \Delta G_x^0 + p\Delta V_x$). Using this method, they were able to identify three regions with distinct sub-global cooperative stabilities and pressure sensitivities [138].

High pressure H/D exchange experiments were also used in the case of the cavity variants of SNase (Fig. 9) showing considerable variations in the measured ΔV_x for the mutants, compared to the flat ΔV_x profile obtained for the pseudo wild type Δ+PHS [31]. In good agreement with equilibrium unfolding data, these H/D experiments revealed a major remodeling of the folding free-energy landscape in response to the introduction of cavity-creating mutations.

5.3. Characterization of the transition state ensemble in the folding reaction

A complete understanding of the protein folding/unfolding phenomenon needs, in addition to the structural description of the different states and their relative population, a temporal description of the sequence of events along the folding pathway. Such a description relies on the measurement of kinetic parameters, after perturbation of the thermodynamic equilibrium between the folded and unfolded conformers of the protein. This perturbation can be achieved by a fast mixing with chaotropic reagent, a pH jump, a temperature jump…and of course a pressure jump (P-jump). In addition to kinetic parameters, these measurements allow the characterization of the transition state expected for a classic first order process, as commonly used to describe an equilibrium reaction between two states. Thus, using pressure to unfold the protein will give access to folding (k_f) and unfolding (k_u) rates, as well as to the volume of the transition state ensemble (TSE): the transition state of a protein being relatively heterogeneous, it is better described as an ensemble of states rather than a unique conformer. In theory, such a description could be reached using the method proposed by Roche et al. [64] described above, based on the analysis of the probability of contacts between residues as determined from the denaturation curves measured at a residue level. Indeed, Fossat et al. [132] successfully used this approach to fully map the entire folding landscape of the leucine rich repeat protein, pp32 (Anp32), combining pressure-dependent site-specific ^{1}H-^{15}N HSQC data with coarse-grained molecular dynamics simulations. The results obtained using this equilibrium approach demonstrate that the main barrier to folding of pp32 is quite broad and lies near the unfolded state, with structure apparent only in the C-terminal region. Nevertheless, this approach, based on steady-state experiments, failed to provide information on the rate constants k_u and k_f associated with the folding process. Such information can only be attained through real-time spectroscopy following a P-Jump [128,139], or, as recently proposed by Zhang et al. [140], through NMR ZZ-exchange Spectroscopy.

5.3.1. P-jump and real-time NMR spectroscopy

The return to a new equilibrium after perturbation can be monitored by different spectroscopic techniques that give access to a "global" measurement of the kinetic parameters for the folding/unfolding reaction (Fluorescence, IR…). A local description of the kinetic parameters and of the transition state ensemble implies the use of a technique combining spatial resolution, allowing a precise local description of the protein, and sufficient time resolution, since the return to thermodynamic equilibrium can be relatively fast (few seconds to few minutes, generally). NMR has good spatial resolution, but its time resolution is limited: the recording time of the 2D [^{1}H-^{15}N] HSQC spectra described above ranges from 10 to 40 min, depending on the sample concentration and the required spectral resolution. Interestingly, the major destabilizing effect of pressure on protein folding equilibrium derives from a large positive activation volume for folding: the activation volume for folding, $\Delta V_f^{\ddagger}$ is usually large and positive (i.e. the molar volume of the transition state ensemble is larger than that of the unfolded states), while the activation volume for unfolding, $\Delta V_u^{\ddagger}$, can be either negative or positive. This slows the folding reaction considerably [141]. In cases for which folding is intrinsically sufficiently slow and folding activation volumes sufficiently large [141,142] pressure-jump can be combined with classical 2D NMR experiments, such as ^{1}H−^{15}N HSQC, to study kinetic mechanisms of folding, yielding folding and unfolding rates for nearly every residue in a protein. Pressure-jump 2D HSQC experiments on staphylococcal nuclease and a series of variants were possible because folding relaxation times at high pressure are extremely slow, ranging between 20 min and 24 h [139]. While conventional HSQC can be readily used for the variants exhibiting the slowest relaxation times (>10 h), measurements performed on the variants with faster relaxation times (<20 min) were performed using 2D SOFAST-HMQC experiments [17,18], recorded in only 25 s. Results from these studies revealed that SNase variants with cavities in the central hydrophobic core showed highly heterogeneous transition-state ensembles, while those containing a cavity in the peripheral region of the protein only showed a slight difference in comparison to the wild type SNase. Additionally, these results further confirmed the more local effect of pressure perturbation as opposed to the global effect of temperature and chemical denaturants [139].

In practice, kinetics measurements consist of recording a series of 2D HSQC (or SOFAST-HMQC) spectra after a pressure jump, in order to correctly sample the exponential decay of the cross-peak intensity during unfolding (in the case of a "positive" P-jump, where pressure is increased) (Fig. 10). Several P-jumps are realized in the pressure range where unfolding appears (typically between 40 and 200 MPa for Δ+PHS SNase and its variants [139]). P-jump

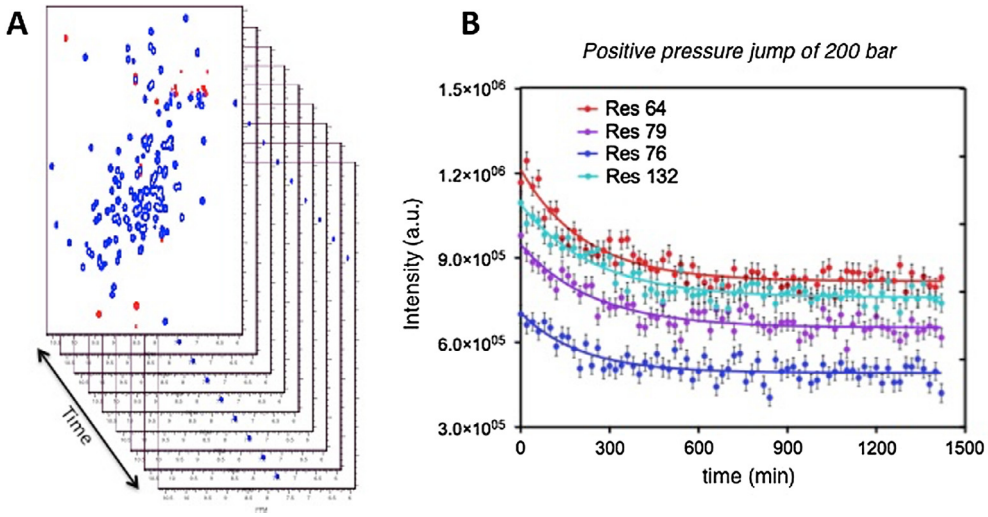

Fig. 10. High Pressure NMR and kinetic measurements. (A) Series of 2D [^{1}H-^{15}N] HSQC spectra used to sample a positive P-jump of 20 MPa (100–120 Mpa) on a sample of Δ+PHS SNase in 2 M GuHCl. The individual measuring time for each HSQC experiment was 20 min, for a protein concentration of 1 mM. (B) Time evolution of the amide cross-peak intensity for 4 representative residues. The curves were obtained by exponential fitting of the intensity values, giving the value of $\tau = 1/(k_u + k_f)$. (from results discussed in [139]).

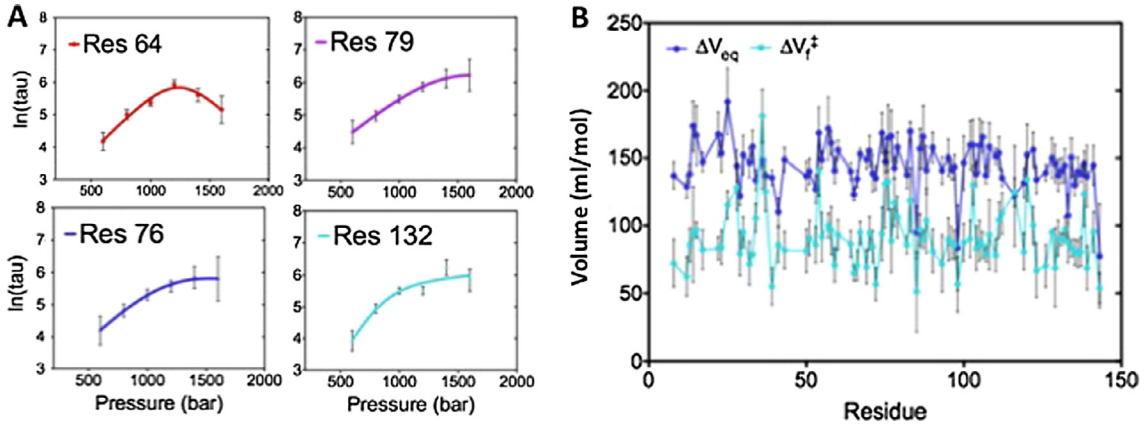

Fig. 11. High-pressure NMR kinetics measurements. (A) Examples for the characteristic "chevron plot" evolution of the residue-specific relaxation time τ values as a function of the final pressure for the pressure jump. Curves are obtained by fitting the experimental values with equation [12] and allow determination of the value of the activation volume for the folding reaction reported by each residue. (B) Comparison of ΔV_{eq} at equilibrium (dark blue) and $\Delta V_f^{\ddagger}$ activation volumes (light blue) as a function of the protein sequence for the variant I92A of Δ+PHS SNase. (Adapted with permission from Roche et al. [139]).

amplitude should be enough to cause a measurable intensity decay for the amide cross peaks, but should remain moderate to avoid any imbalance between the folding and the unfolding reactions: an excessive positive P-jump, for instance, will favor the unfolding reaction at the expense of the folding reaction. For instance, for Δ+PHS SNase and its variants, pressure jumps of 20 MPa were used, which is about 10 per cent of the pressure range needed to fully unfold the proteins (200 MPa) [139].

The fit of the amide cross-peak decays with exponential functions gives a residue-specific exponential time τ for each P-jump, equal to the inverse of the sum of the folding and unfolding rates ($\tau_{(p)} = 1/(k_u + k_f)$). It is thus possible to obtain the value of the activation volume (TSE volume) for the unfolding reaction at atmospheric pressure by the fit of the evolution of τ values at different pressure with the following equation:

$$\tau(p) = \left[k_{u0} e^{\left(\frac{-p\Delta V_{u0}^{\ddagger}}{RT}\right)} + k_{u0} K_{eq} e^{\left(\frac{-p(\Delta V_{eq} + \Delta V_{u0}^{\ddagger})}{RT}\right)} \right]^{-1} \quad (12)$$

$$k_f(p) = k_{f0} e^{-p\Delta V_f^{\ddagger}/RT} \quad \text{and} \quad k_u(p) = k_{u0} e^{-p\Delta V_u^{\ddagger}/RT} \quad (13)$$

where $\Delta V_{eq} = \Delta V_f - \Delta V_u$ and $K_{eq} = k_f/k_u$ stand for the volume difference between the folded and unfolded states and the equilibrium constant measured at thermodynamic equilibrium. Only two variables need to be fitted: k_{u0} (the unfolded rate at atmospheric pressure) and $\Delta V_{u0}^{\ddagger}$ (the activation volume for unfolding at atmospheric pressure) (Fig. 11).

5.3.2. Kinetics parameters through NMR ZZ-exchange spectroscopy

The obvious limitation of the method presented above for obtaining kinetic parameters for the folding reaction is the low time resolution of 2D NMR spectroscopy, even though this drawback has been at least partially circumvented by recent methodological developments [143,144]: HSQC-type experiments can now be recorded in less than a minute, significantly extending the application of real-time spectroscopy. The approach remains unsatisfactory for studying folding kinetics for proteins with sub-second relaxation times, which is the case for most small globular proteins that fold rather quickly, many on time scales of milliseconds or even less. For a protein with a folding time of 1 ms ($k_f = 1000\ s^{-1}$) at atmospheric pressure, and a positive activation volume of 100 mL/mol, folding will be slowed to a folding time

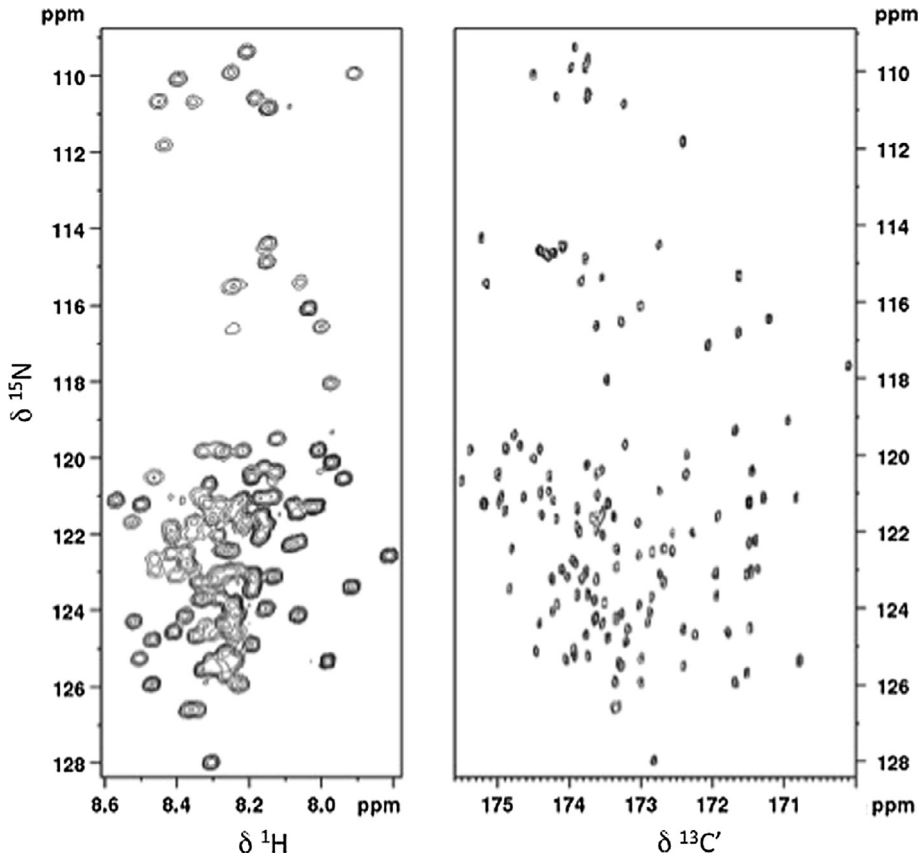

Fig. 12. If two-dimensional heteronuclear correlation spectra provide the foundation for all biomolecular NMR studies, traditional ^{1}H-detected methods do not work as well for IDPs (including unfolded states) as newer ^{13}C-detected methods. [^{1}H,^{15}N] HSQC Spectrum (left) and [^{13}C,^{15}N] CON recorded on a sample of Δ+PHS SNase at 250 MPa and in presence of 1.8 M of GuHCl.

of about 1 min at a pressure of 2500 bar. Unfortunately, this time scale still remains too fast for acquisition of classical 2D NMR spectra as a function of time. However, conformational exchange phenomena that are slow on the NMR time scale (100 ms to ~1 s) can be accurately quantified by 2D exchange NMR [140]. One such approach to quantifying chemical exchange is provided by ZZ-exchange spectroscopy, which was first used to determine tyrosine ring flipping [145] and was later extended to measure the folding and unfolding rates of the N-terminal SH3 domain of the protein Drk [146,147]. By combining the effect of high pressure with the ZZ-exchange NMR method, Zhang et al. [140] were able to obtain residue-specific folding rates for the two autonomous N-terminal and C-terminal domains of the ribosomal protein L9, indicating that N-terminal (NTL9) folding is a two-state process. Large positive activation volumes for folding were reported for both NTL9 and CTL9, indicating that their transition states still contain the majority of the solvent-excluded voids found in the cores of the native ensembles [140].

5.4. Characterization of protein unfolded states

A structural interpretation of the thermodynamic stability of proteins requires an understanding of the structural properties of the unfolded state. However, the structural properties of the denatured state achieved may depend upon the method employed to perturb the native structure. Using SAXS and FT-IR measurements, several authors [45,46] showed that application of high pressure up to 300 MPa to SNase leads to an approximate twofold increase of the Rg value and a large broadening of the pair-distance-distribution function, indicating a transition from a globular to an ellipsoidal chain structure but still far from being an extended random coil. Interestingly, the denatured states achieved by urea as denaturant lead to a similar value for the radius of gyration. Analysis of the FT-IR spectral components reveals that the pressure-induced denaturation is accompanied by an increase in disordered and turn structures while the content of β-sheets and α-helices drastically decreases. Nonetheless, the pressure-induced denatured state above 300 MPa retains some degree of β-like secondary structure and the molecule cannot be described as a fully extended random coil. Temperature-induced denaturation involves a further unfolding of the protein molecule, which is indicated by a larger Rg and significantly lower fractional intensities of IR bands associated with β-sheet secondary structure elements. In contrast to the pressure-denatured SNase, the thermally denatured state can be described by a more extended, possibly bimodal structure with a very low content of secondary structure elements. Thus, these data indicated that thermal denaturation leads to a more disrupted structure than is achieved by pressure.

Remarkably, unfolded proteins are similar to intrinsically disordered proteins (IDPs), a large class of eukaryotic proteins that remains intrinsically disordered in their native states [148–151]. Nuclear magnetic resonance (NMR) spectroscopy is probably the most powerful biophysical tool for studying IDPs due to the remarkable sensitivity of different NMR phenomena to dynamics occurring on time scales varying from picoseconds to hours, and the ability to report on both local and long-range structure [152]. In particular, residual dipolar couplings (RDCs), which become measurable when a protein is dissolved in an anisotropic alignment medium or matrix [153,154], have been shown to be very sensitive reporters of local and long-range structure [155] even

in highly disordered systems [156]. Since the initial demonstration that RDCs can be measured in proteins even under highly denaturing conditions [157–165], it has been recognized that RDCs provide unique site-specific probes of orientational order in disordered states [156,166]. Residual dipolar couplings (RDC) represent also a promising strategy for the characterization of high-pressure conformational substates. Several groups have shown that various alignment media, including Pf1 filamentous phage, C12E5/n-hexanol mixture and dinucleotide d(GpG), can be used to measure RDCs in high-pressure conditions [167–169]. RDCs measured at 600 bar in a weakly oriented solution obtained by the addition of squalamine were recently used as restraints in all-atom molecular dynamics simulations in order to characterize the pressure-induced structural changes in the mature HIV-1 Protease [170].

Of course, the limiting step of these studies remains the assignment of the NMR spectra of the unfolded protein. The intrinsically small range of proton chemical shifts in unfolded systems typically leads to severe resonance overlap. The high-pressure ZZ-exchange experiments quoted above can provide a relatively easy method to assign the $^{1}H/^{15}N$ chemical shifts of the pressure-induced denatured states in the case of proteins of moderate molecular weight [140]. But conformational exchange and also exchange with solvent in the case of amide protons can also broaden the proton resonances beyond detection, especially at physiological pH. By contrast, heteronuclear chemical shifts, which are not sensitive to solvent exchange, have a much larger chemical shift dispersion even in the absence of any stable 3D structure, and provide an ideal tool to characterize these systems [171,172] (Fig. 12). Other technical aspects in favor of heteronuclear direct detection include the absence, in general, of intense solvent signals that need to be suppressed and a reduced sensitivity to high ionic strength (high salt concentrations) that may cause problems for proton detection. Therefore, heteronuclear NMR experiments based on ^{13}C direct detection provide new tools complementing or replacing the standard ^{1}H-detected experiments, especially in the case of disordered systems.

6. Conclusion

Pressure perturbation offers unique opportunities to finely tune the stability of a globular protein or to modulate the rate of a conformational exchange in a completely reversible manner. The spatial and temporal resolution of NMR spectroscopy is necessary to describe the folding pathway at a residue-specific level, giving a description of the pathway both in structural terms, bringing to light the existence of intermediate states, and in dynamic terms, revealing rates of local rearrangements involved.

Beside the fundamental interest of studying the protein folding/unfolding mechanism, a better understanding of this phenomenon will find applications in many fields. Is it important to recall that the so-called "conformational" neurodegenerative diseases (Alzheimer, Parkinson, prion diseases...) are due to misfolding of proteins? A better understanding of the folding/unfolding mechanism for each of these specific proteins may allow exploration of new avenues for drug rational design. Similarly, understanding the phenomena underlying protein stability is a major issue for the design of industrial enzymes or other biotechnological products that can function at high pressure or high temperature. Thus, understanding how a protein can accommodate mutations to gain stability, keeping its function intact, has a major economic impact. The challenge is great, but combining NMR with high pressure has already proven to be an extremely powerful approach in this particular field, providing rigorous answers to difficult and important questions.

Acknowledgements

This work was supported by French Infrastructure for Integrated Structural Biology grant No. ANR-10-INSB-05-01 (C.R.), the Roy J. Carver Foundation (J.R), and NSF MCB-1514575 (C.A.R.).

References

[1] C.B. Anfinsen, Principles that govern the folding of protein chains, Science 181 (1973) 223–230.
[2] A.D. Robertson, R.L. Baldwin, Hydrogen exchange in thermally denatured ribonuclease A, Biochemistry 30 (1991) 9907–9914.
[3] D.M. Korzhnev, X. Salvatella, M. Vendruscolo, A.A. Di Nardo, A.R. Davidson, C. M. Dobson, L.E. Kay, Low-populated folding intermediates of Fyn SH3 characterized by relaxation dispersion NMR, Nature 430 (2004) 586–590.
[4] T.L. Religa, J.S. Markson, U. Mayor, S.M.V. Freund, A.R. Fersht, Solution structure of a protein denatured state and folding intermediate, Nature 437 (2005) 1053–1056.
[5] X. Salvatella, C.M. Dobson, A.R. Fersht, M. Vendruscolo, Determination of the folding transition states of barnase by using phi(I)-value-restrained simulations validated by double mutant phi(IJ)-values, Proc. Natl. Acad. Sci. U.S.A. 102 (2005) 12389–12394.
[6] J. Gsponer, H. Hopearuoho, S.B. Whittaker, G.R. Spence, G.R. Moore, E. Paci, S.E. Radford, M. Vendruscolo, Determination of an ensemble of structures representing the intermediate state of the bacterial immunity protein Im7, Proc. Natl. Acad. Sci. U.S.A. 103 (2006) 99–104.
[7] P. Neudecker, A. Zarrine-Afsar, A.R. Davidson, L.E. Kay, Phi-value analysis of a three-state protein folding pathway by NMR relaxation dispersion spectroscopy, Proc. Natl. Acad. Sci. U.S.A. 104 (2007) 15717–15722.
[8] N. Calosci, C.N. Chi, B. Richter, C. Camilloni, A. Engström, L. Eklund, C. Travaglini-Allocatelli, S. Gianni, M. Vendruscolo, P. Jemth, Comparison of successive transition states for folding reveals alternative early folding pathways of two homologous proteins, Proc. Natl. Acad. Sci. U.S.A. 105 (2008) 19241–19246.
[9] C.T. Friel, D.A. Smith, M. Vendruscolo, J. Gsponer, S.E. Radford, The mechanism of formation of a folding intermediate reveals the competition between functional and kinetic evolutionary constraints, Nat. Struct. Mol. Biol. 16 (2009) 318–324.
[10] H. Roder, K. Maki, H. Cheng, Early events in protein folding explored by rapid mixing methods, Chem. Rev. 106 (2006) 1836–1861.
[11] A.I. Bartlett, S.E. Radford, An expanding arsenal of experimental methods yields an explosion of insights into protein folding mechanism, Nat. Struct. Mol. Biol. 16 (2009) 582–588.
[12] J.N. Onuchic, P.G. Wolynes, Theory of protein folding, Curr. Opin. Struct. Biol. 14 (2004) 70–75.
[13] K.A. Dill, S.B. Ozkan, M.S. Shell, T.R. Weikl, The protein folding problem, Annu. Rev. Biophys. 37 (2008) 289–316.
[14] K. Lindorff-Larsen, S. Piana, R.O. Dror, D.E. Shaw, How fast-folding proteins fold, Science 334 (2011) 517–520.
[15] D.M. Korzhnev, L.E. Kay, Probing invisible, low-populated states of protein molecules by relaxation dispersion NMR spectroscopy: an application to protein folding, Acc. Chem. Res. 41 (2008) 442–451.
[16] M. Zeeb, J. Balbach, Protein folding studied by real-time NMR spectroscopy, Methods 34 (2004) 65–74.
[17] P. Schanda, B. Brutscher, Very fast two-dimensional NMR spectroscopy for real-time investigation of dynamic events in proteins on the time scale of seconds, J. Am. Chem. Soc. 127 (2005) 8014–8015.
[18] P. Schanda, V. Forge, B. Brutscher, Protein folding and unfolding studied at atomic resolution by fast two-dimensional NMR spectroscopy, Proc. Natl. Acad. Sci. U.S.A. 104 (2007) 11257–11262.
[19] M.M.G. Krishna, L. Hoang, Y. Lin, S.W. Englander, Hydrogen exchange methods to study protein folding, Methods 34 (2004) 51–64.
[20] Y. Bai, Protein folding pathways studied by pulsed- and native state hydrogen exchange, Chem. Rev. 106 (2006) 1757–1768.
[21] S.W. Englander, L. Mayne, M.M.G. Krishna, Protein folding and misfolding: mechanism and principles, Q. Rev. Biophys. 40 (2007) 287–326.
[22] P.W. Bridgman, The coagulation of albumin by pressure, J. Biol. Chem. 19 (1914) 511–512.
[23] Y.O. Kamatari, R. Kitahara, H. Yamada, S. Yokoyama, K. Akasaka, High-pressure NMR spectroscopy for characterizing folding intermediates and denatured states of proteins, Methods 34 (2004) 133–143.
[24] K. Akasaka, R. Kitahara, Y.O. Kamatari, Exploring the folding energy landscape with pressure, Arch. Biochem. Biophys. 531 (2013) 110–115.
[25] W. Kauzmann, Some factors in the interpretation of protein denaturation, Adv. Protein Chem. 14 (1959) 1–63.
[26] P.L. Privalov, S.J. Gill, Stability of protein structure and hydrophobic interaction, Adv. Protein Chem. 39 (1988) 191–234.
[27] K.P. Murphy, P.L. Privalov, S.J. Gill, Common features of protein unfolding and dissolution of hydrophobic compounds, Science 247 (1990) 559–561.
[28] C.A. Royer, Revisiting volume changes in pressure-induced protein unfolding, Biochem. Biophys. Acta 1595 (2002) 201–209.
[29] C.A. Royer, Why and how does pressure unfold proteins?, Subcell Biochem. 72 (2015) 59–71.

[30] J. Rouget, T. Aksel, J. Roche, J. Saldana, A.E. Garcia, D. Barrick, C.A. Royer, Size and sequence and the volume change of protein folding, J. Am. Chem. Soc. 133 (2011) 6020–6027.

[31] J. Roche, M. Dellarole, J.A. Caro, E. Guca, D.R. Norberto, Y.-S. Yang, A.E. Garcia, C. Roumestand, B. García-Moreno, C.A. Royer, Remodeling of the folding free-energy landscape of staphylococcal nuclease by cavity-creating mutations, Biochemistry 51 (2012) 9535–9546.

[32] J.D. Bryngelson, J.N. Onuchic, N.D. Socci, P.G. Wolynes, Funnels, pathways, and the energy landscape of protein folding: a synthesis, Proteins 21 (1995) 167–195.

[33] J.N. Onuchic, P.G. Wolynes, Z. Luthey-Schulten, N.D. Socci, Toward an outline of the topography of a realistic protein folding funnel, Proc. Natl. Acad. Sci. U. S.A. 92 (1995) 3626–3630.

[34] S.A. Hawley, Reversible pressure-temperature denaturation of chymotrypsinogen, Biochemistry 10 (1971) 2426–2442.

[35] J.F. Brandts, R.J. Oliveira, C. Westort, Thermodynamics of protein denaturation. Effect of pressure on the denaturation of Ribonuclease A, Biochemistry 9 (1970) 1038–1047.

[36] H. Lesh, C. Hecht, J. Friedrich, Protein phase diagrams: the physics behind their elliptic shape, J. Chem. Phys. 121 (2004) 12671–12675.

[37] L. Smeller, Pressure–temperature phase diagrams of biomolecules, Biochem. Biophys. Acta 1595 (2002) 11–29.

[38] R. Ravindra, R. Winter, On the temperature-pressure free-energy landscape of proteins, Chem. Phys. Chem. 4 (2003) 359–365.

[39] F. Meersman, L. Smeller, K. Heremans, Protein stability and dynamics in the pressure-temperature plane, Biochem. Biophys. Acta 1764 (2006) 346–354.

[40] A. Yamaguchi, T.H. Yamada, K. Akasaka, Thermodynamics of unfolding of ribonuclease A under high pressure. A study by proton NMR, J. Mol. Biol. 250 (1995) 689–694.

[41] R. Winter, W. Dzwolak, Exploring the temperature-pressure configurational landscape of biomolecules: from lipid membranes to proteins, Phil. Trans. R. Soc. A 363 (2005) 547–563.

[42] F. Meersman, C.M. Dobson, Probing the pressure-temperature stability of amyloid fibrils provides new insights into their molecular properties, Biochem. Biophys. Acta 1764 (2006) 452–460.

[43] K. Goossens, J. Haelewyn, F. Meersman, M. De Ley, K. Heremans, Pressure- and temperature-induced unfolding and aggregation of recombinant interferon-γ: a Fourier transform infrared spectroscopy study, Biochem. J. 370 (2003) 529–535.

[44] V.Y. Griko, V.P. Kutyshenko, Differences in the process of β-lactoglobulin cold and heat denaturations, Biophys. J. 67 (1994) 356–363.

[45] G. Panick, R. Malessa, R. Winter, G. Rapp, K.J. Frye, C.A. Royer, Structural characterization of the pressure-denatured state and unfolding/refolding kinetics of staphylococcal nuclease by synchrotron small-angle X-ray scattering and fourier-transform infrared spectroscopy, J. Mol. Biol. 275 (1998) 389–402.

[46] M.A. Schroer, M. Paulus, C. Jeworrek, C. Krywka, S. Schmacke, Y. Zhai, F.D.C. Wieland, C.J. Sahle, M. Chimenti, C.A. Royer, B. Garcia-Moreno, M. Tolan, R. Winter, High-pressure SAXS study of folded and unfolded ensembles of proteins, Biophys. J. 99 (2010) 3430–3437.

[47] F. Meersman, L. Smeller, K. Heremans, Comparative Fourier transform infrared spectroscopy study of cold-, pressure- and heat-induced unfolding and aggregation of myoglobin, Biophys. J. 82 (2002) 2635–2644.

[48] L. Smeller, F. Meersman, K. Heremans, Refolding studies using pressure: the folding landscape of lysozyme in the pressure-temperature plane, Biochem. Biophys. Acta 1764 (2006) 497–505.

[49] J. Zhang, X. Peng, A. Jonas, J. Jonas, NMR study of the cold, heat, and pressure unfolding of ribonuclease A, Biochemistry 34 (1995) 8361–8641.

[50] M.W. Lassalle, H. Yamada, K. Akasaka, The pressure-temperature free energy-landscape of Staphylococcal nuclease monitored by ^{1}H NMR, J. Mol. Biol. 298 (2000) 293–302.

[51] H. Herberhold, R. Winter, Temperature and pressure induced unfolding of ubiquitin, J. Phys.: Condens. Matter 14 (2002) 11485–11488.

[52] H. Herberhold, S. Marchal, R. Lange, C.H. Scheyhing, R.F. Vogel, R. Winter, Characterization of the pressure-induced intermediate and unfolded states of red-shifted Green Fluorescent Protein. A static and kinetic FTIR, UV/VIS and fluorescence spectroscopy study, J. Mol. Biol. 330 (2003) 1153–1164.

[53] H. Lesh, H. Stadlbauer, J. Friedrich, J.M. Vanderkooi, Stability diagram and unfolding of a modified cytochrome c: what happens in the transformation regime?, Biophys J. 82 (2002) 1644–1653.

[54] J. Wiedersich, S. Kohler, A. Skerra, J. Friedrich, Temperature and pressure dependence of protein stability: the engineered fluorescein-binding lipocalin FluA shows and elliptic phase diagram, Proc. Natl. Acad. Sci. U.S.A. 105 (2008) 5756–5761.

[55] A. Maeno, H. Matsuo, K. Akasaka, The pressure-temperature phase diagram of hen lysozyme at low pH, Biophysics (Nagoya-shi) 5 (2009) 1–9.

[56] G. Panick, G.J.A. Vidgurigis, R. Malessa, G. Rapp, R. Winter, C.A. Royer, Exploring the temperature-pressure phase diagram of Staphylococcal nuclease, Biochemistry 38 (1999) 4157–4164.

[57] J.R. Grigera, A.N. McCarthy, The behavior of the hydrophobic effect under pressure and protein denaturation, Biophys. J. 98 (2010) 1626–1631.

[58] L.N. Lin, J.F. Brandts, J.M. Brandts, V. Plotnikov, Determination of the volumetric properties of proteins and other solutes using pressure perturbation calorimetry, Anal. Biochem. 302 (2002) 144–160.

[59] L. Mitra, J.B. Rouget, B. Garcia-Moreno, C.A. Royer, R. Winter, Towards a quantitative understanding of protein hydration and volumetric properties, ChemPhysChem 9 (2008) 2715–2721.

[60] C.R. Chen, G.I. Makhatadze, Molecular determinant of the effects of hydrostatic pressure on protein folding stability, Nat. Commun. 8 (2017) 14561.

[61] K. Heremans, High pressure effects on proteins and other biomolecules, Annu. Rev. Biophys. Bioeng. 11 (1982) 1–21.

[62] J.L. Silva, G. Weber, Pressure stability of proteins, Annu. Rev. Phys. Chem. 44 (1993) 89–113.

[63] J.L. Silva, D. Foguel, C.A. Royer, Pressure provides new insights into protein folding, dynamics and structure, Trends Biochem. Sci. 26 (2001) 612–618.

[64] J. Roche, J.A. Caro, D.R. Norberto, P. Barthe, C. Roumestand, J.L. Schlessman, A. E. Garcia, B. Garcia-Moreno, C.A. Royer, Cavities determine the pressure unfolding of proteins, Proc. Natl. Acad. Sci. U.S.A. 109 (2012) 6945–6950.

[65] N. Ando, B. Barstow, W.A. Baase, A. Fields, B.W. Matthews, S.M. Gruner, Structural and thermodynamic characterization of T4 lysozyme mutants and the contribution of internal cavities to pressure denaturation, Biochemistry 47 (2008) 11097–11109.

[66] G. Hummer, S. Garde, A.E. García, M.E. Paulaitis, L.R. Pratt, The pressure dependence of hydrophobic interactions is consistent with the observed pressure denaturation of proteins, Proc. Natl. Acad. Sci. U.S.A. 95 (1998) 1552–1555.

[67] L. Mitra, K. Hata, R. Kono, A. Maeno, D. Isom, J.B. Rouget, R. Winter, K. Akasaka, B. García-Moreno, C.A. Royer, V(i)-value analysis: a pressure-based method for mapping the folding transition state ensemble of proteins, J. Am. Chem. Soc. 129 (2007) 14108–14109.

[68] L. Brun, D.G. Isom, P. Velu, B. García-Moreno, C.A. Royer, Hydration of the folding transition state ensemble of a protein, Biochemistry 45 (2006) 3473–3480.

[69] A.D. Tsamaloukas, N.K. Pyzocha, G.I. Makhatadze, Pressure perturbation calorimetry of unfolded proteins, J. Phys. Chem. B. 114 (2010) 16166–16170.

[70] D. Vasilchuk, P.P. Pandharipande, S. Suladze, J.M. Sanchez-Ruiz, G.I. Makhatadze, Molecular determinants of expansivity of native globular proteins: a pressure perturbation calorimetry study, J. Phys. Chem. B. 118 (2014) 6117–6122.

[71] M. Dellarole, J.A. Caro, J. Roche, M. Fossat, P. Barthe, B. García-Moreno, C.A. Royer, C. Roumestand, Evolutionarily conserved pattern of interactions in a protein revealed by local thermal expansion properties, J. Am. Chem. Soc. 137 (2015) 9354–9362.

[72] N. Good, D. Winget, W. Winter, T. Connolly, S. Irawa, R. Singh, Hydrogen ion buffers for biological research, Biochemistry 5 (1966) 467–477.

[73] R.C. Neuman, W. Kauzmann, A. Zipp, Pressure-dependence of weak acid ionization in aqueous buffers, J. Phys. Chem. 77 (1973) 2687–2691.

[74] A.L. Surdo, K. Bernstrom, C.A. Jonsson, F.J. Millero, Molar volume and adiabatic compressibility of aqueous phosphate solutions at 25 C, Phys. Chem. 83 (1979) 1255–1262.

[75] Y. Kitamura, T. Itoh, Reaction volume of protonic ionization forbuffering agents—prediction of pressure-dependence of pH and pOH, J. Solution Chem. 16 (1987) 715–725.

[76] M. Hayert, J.M. Perrier-Cornet, P. Gervais, A simple method for measuring the pH of acid solutions under high pressure, J. Phys. Chem. A 103 (1999) 1785–1789.

[77] V. Orlien, K. Olsen, L.H. Skibsted, In situ measurements of pH changes in beta-lactoglobulin solutions under high hydrostatic pressure, J. Agric. Food Chem. 55 (2007) 4422–4428.

[78] M. Salerno, J.J. Ajimo, J.A. Dudley, K. Binzel, P. Urayama, Characterization of dual-wavelength seminaphthofluorescein and seminaphthorhodafluor dyes for pH sensing under high hydrostatic pressures, Anal. Biochem. 362 (2007) 258–267.

[79] H.M. De Pedro, P. Urayama, Using LysoSensor Yellow/Blue DND-160 to sense acidic pH under high hydrostatic pressures, Anal. Biochem. 384 (2009) 359–361.

[80] R.J. Quinlan, G.D. Reinhart, Baroresistant buffer mixtures for biochemical analyses, Anal. Biochem. 341 (2005) 69–76.

[81] V.M. Balasubramanian, E.Y. Ting, C.M. Stewart, J.A. Robbins, Recommended laboratory practices for conducting high-pressure microbial inactivation experiments, Innov. Food Sci. Emerg. Technol. 5 (2004) 299–306.

[82] E. Gayán, S. Condón, I. Álvarez, M. Nabakabaya, B. Mackey, Effect of pressure-induced changes in the ionization equilibria of buffers on inactivation of Escherichia coli and Staphylococcus aureus by high hydrostatic Pressure, Appl. Environ. Microbiol. 13 (2013) 4041–4047.

[83] G.B. Benedek, E.M. Purcell, Nuclear magnetic resonance in liquids under high pressure, J. Chem. Phys. 22 (1954) 2003–2012.

[84] L. Ballard, C. Reiner, J. Jonas, High-resolution NMR probe for experiments at high-pressures, J. Magn. Res. 123 (1996) 81–86.

[85] L. Ballard, A. Yu, C. Reiner, J. Jonas, A high-pressure, high-resolution NMR probe for experiments at 500 MHz, J. Magn. Res. 133 (1998) 190–193.

[86] J. Jonas, High-resolution nuclear magnetic resonance studies of proteins, Biochem. Biophys. Acta 1595 (2002) 145–159.

[87] H. Yamada, Pressure-resisting glass cell for high-pressure, high resolution NMR measurements, Rev. Sci. Instrum. 45 (1974) 640–642.

[88] H. Yamada, K. Nishikawa, M. Honda, T. Shimura, K. Akasaka, K. Tabayashi, Pressure-resisting cell for high-pressure, high-resolution nuclear magnetic resonance measurements at very high magnetic fields, Rev. Sci. Instrum. 72 (2001) 1463–1471.

[89] K. Akasaka, Probing conformational fluctuations of proteins by pressure perturbation, Chem. Rev. 106 (2006) 1814–1835.
[90] M.W. Lassalle, K. Akasaka, The use of high-pressure nuclear magnetic resonance to study protein folding, Methods Mol. Biol. 350 (2007) 21–38.
[91] K. Akasaka, High pressure NMR spectroscopy, Subcell. Biochem. 72 (2015) 707–721.
[92] J.L. Urbauer, M.R. Ehrhardt, R.J. Bieber, P.F. Flynn, J.A. Wand, High-resolution triple-resonance NMR steptroscopy of a novel calmodulin-peptide complex at kilobar pressures, J. Am. Chem. Soc. 118 (1996) 11329–11330.
[93] M.R. Arnold, H.R. Kalbitzer, W. Kremer, High-sensitivity sapphire cells for high pressure NMR spectroscopy on proteins, J. Magn. Res. 161 (2003) 127–131.
[94] M.B. Erlach, C.E. Munte, W. Kremer, R. Hartl, D. Rochelt, D. Niesner, H.R. Kalbitzer, Ceramics cells for high pressure NMR spectroscopy of proteins, J. Magn. Res. 204 (2010) 196–199.
[95] R.W. Peterson, J.A. Wand, Self-contained high-pressure cell, apparatus, and procedure for the preparation of encapsulated proteins dissolved in low viscosity fluids for nuclear magnetic resonance spectroscopy, Rev. Sci. Instrum. 76 (2005) 094101.
[96] J. Roche, J.A. Caro, M. Dellarole, E. Guca, C.A. Royer, B. García-Moreno, A.E. Garcia, C. Roumestand, Structural, energetic and dynamic responses of the native state ensemble of staphylococcal nuclease to cavity-creating mutations, Proteins 81 (2013) 1069–1080.
[97] N.J. Baxter, L.L.P. Hosszu, J.P. Waltho, M.P. Williamson, Characterisation of low free-energy excited states of folded proteins, J. Mol. Biol. 284 (1998) 1625–1639.
[98] K. Akasaka, H. Li, Low-lying excited states of proteins revealed from nonlinear pressure shifts in ^{1}H and ^{15}N NMR, Biochemistry 40 (2001) 8665–8671.
[99] R. Kitahara, H. Yamada, K. Akasaka, Two folded conformers of ubiquitin revealed by high-pressure NMR, Biochemistry 40 (2001) 13556–13563.
[100] R. Kitahara, S. Yokoyama, K. Akasaka, NMR snapshots of a fluctuating protein structure: ubiquitin at 30 bar–3 kbar, J. Mol. Biol. 347 (2005) 277–285.
[101] G. Nielsen, H.R.A. Jonker, N. Vajpai, S. Grzesiek, H. Schwalbe, Kinase in motion: insights into the dynamic nature of p38a by high-pressure NMR spectroscopic studies, Chem. Bio. Chem. 14 (2013) 1799–1806.
[102] R. Kitahara, K. Akasaka, Close identity of a pressure-stabilized intermediate with a kinetic intermediate in protein folding, Proc. Natl. Acad. Sci. U.S.A. 100 (2003) 3167–3172.
[103] H. Li, K. Akasaka, Conformational fluctuations of proteins revealed by variable pressure NMR, Biochem. Biophys. Acta 1764 (2006) 331–345.
[104] G. Wagner, A. Pardi, K. Wuthrich, Hydrogen bond length and proton NMR chemical shifts in proteins, J. Am. Chem. Soc. 105 (1983) 5948–5949.
[105] D. Sitkoff, D.A. Case, Theories of chemical shift anisotropies in proteins and nucleic acids, Prog. Nucl. Magn. Reson. Spectrosc. 32 (1998) 165–190.
[106] L. Nisius, S. Grzesiek, Key stabilizing elements of protein structure identified through pressure and temperature perturbation of its hydrogen bond network, Nat. Chem. 4 (2012) 711–717.
[107] D.J. Wilton, R. Kitahara, K. Akasaka, M.P. Williamson, Pressure-dependent ^{13}C chemical shifts in proteins: origins and applications, J. Biomol. NMR 44 (2009) 25–33.
[108] R. Kitahara, K. Hata, H. Li, M.P. Williamson, K. Akasaka, Pressure-induced chemical shifts as probes for conformational fluctuations in proteins, Prog. Nucl. Magn. Reson. Spectrosc. 71 (2013) 35–58.
[109] G.I. Penna, Y. Mori, R. Kitahara, K. Akasaka, Y. Okamoto, Modeling ^{15}N NMR chemical shift changes in protein backbone with pressure, J. Chem. Phys. 145 (2016) 085104–085112.
[110] M.R. Arnold, W. Kremer, H.-D. Lüdemann, H.R. Kalbitzer, ^{1}H-NMR parameters of common amino acid residues measured in aqueous solutions of the linear tetrapeptides Gly-Gly-X-Ala at pressures between 0.1 and 200 MPa, Biophys. Chem. 96 (2002) 129–140.
[111] J. Koehler, M.B. Erlach, E. Crusca, W. Kremer, C.E. Munte, H.R. Kalbitzer, Pressure dependence of ^{15}N chemical shifts in model peptides Ac-Gly-Gly-X-Ala-NH_2, Materials 5 (2012) 1774–1786.
[112] M.B. Erlach, J. Koehler, E. Crusca, W. Kremer, C.E. Munte, H.R. Kalbitzer, Pressure dependence of backbone chemical shifts in the model peptides Ac-Gly-Gly-Xxx-Ala-NH_2, J. Biomol. NMR 65 (2016) 65–77.
[113] R. Frach, P. Kibes, S. Böttcher, T. Pongratz, S. Strohfeldt, S. Kurrmann, J. Koehler, M. Hofmann, W. Kremer, H.R. Kalbitzer, O. Reiser, D. Horinek, S.M. Kast, The chemical shift baseline for high-pressure NMR spectra of proteins, Angew. Chem. Int. Ed. 55 (2016) 8757–8760.
[114] M.B. Erlach, J. Koehler, B. Moeser, D. Horinek, W. Kremer, H.R. Kalbitzer, Relationship between nonlinear pressure-induced chemical shift changes and thermodynamic parameters, J. Phys. Chem. B 118 (2014) 5681–5690.
[115] S.P. Narayanan, D.G. Nair, D. Schaal, M.B.d. Aguiar, S. Wenzel, W. Kremer, S. Schwarzinger, H.R. Kalbitzer, Structural transitions in full-length human prion protein detected by xenon as probe and spin labeling of the N-terminal domain, Sci. Rep. 6 (2016) 28419.
[116] H.Y.K. Inoue, K. Akasaka, C. Herrmann, W. Kremer, T. Maurer, R. Döker, H.R. Kalbitzer, Pressure-induced local unfolding of the Ras binding domain of RalGDS, Nat. Struct. Biol. 7 (2000) 547–550.
[117] K. Kuwata, H. Li, H. Yamada, G. Legname, S.B. Prusiner, K. Akasaka, T.L. James, Locally disordered conformer of the hamster prion protein: a crucial intermediate to PrPSc, Biochemistry 41 (2002) 12277–12283.
[118] G.J.A. Vidugiris, C.A. Royer, Determination of the volume changes for pressure-induced transitions of apomyoglobin between the native, molten globule, and unfolded states, Biophys. J. 75 (1998) 463–470.
[119] R. Kitahara, A.K. Simorellis, K. Hata, A. Maeno, S. Yokoyama, S. Koide, K. Akasaka, A delicate interplay of structure, dynamics, and thermodynamics for function: a high pressure NMR study of outer surface protein A, Biophys. J. 102 (2012) 916–926.
[120] K. Kuwata, H. Li, H. Yamada, C.A. Batt, Y. Goto, K. Akasaka, High-pressure NMR reveals a variety of fluctuating conformers in β-lactoglobulin, J. Mol. Biol. 305 (2001) 1073–1083.
[121] L. Ragona, F. Fogolari, S. Romagnoli, L. Zetta, J.L. Maubois, H. Molinari, Unfolding and refolding of bovin β-lactoglobulin monitored by hydrogen exchange measurements, J. Mol. Biol. 293 (1999) 953–969.
[122] M.P. Williamson, K. Akasaka, M. Refaee, The solution structure of bovine pancreatic trypsin inhibitor at high pressure, Protein Sci. 12 (2003) 1971–1979.
[123] M. Refaee, T. Tezuka, K. Akasaka, M.P. Williamson, Pressure-dependent changes in the solution structure hen egg-white lysozyme, J. Mol. Biol. 327 (2003) 857–865.
[124] S. Kitazawa, T. Kameda, M. Yagi-Utsumi, K. Sugase, N.J. Baxter, K. Kato, M.P. Williamson, R. Kitahara, Solution structure of the Q41N variant of ubiquitin as a model for the alternatively folded N2 state of ubiquitin, Biochemistry 52 (2013) 1874–1885.
[125] R. Day, A.E. Angel, Water penetration in the low and high-pressure native states of ubiquitin, Proteins 70 (2008) 1175–1184.
[126] T. Imai, S. Ohyama, A. Kovalenko, F. Hirata, Theoretical study of the partial molar volume change associated with the pressure-induced structural transition of ubiquitin, Protein Sci. 16 (2007) 1927–1933.
[127] M.O. Lindberg, M. Oliveberg, Malleability of protein folding pathways: a simple reason for complex behaviour, Curr. Opin. Struct. Biol. 17 (2007) 21–29.
[128] J. Roche, M. Dellarole, C.A. Royer, C. Roumestand, Exploring the protein folding pathway with high-pressure NMR: steady-state and kinetics studies, Subcell. Biochem. 72 (2015) 261–278.
[129] J.M. Louis, J. Roche, Evolution under drug pressure remodels the folding free-energy landscape of mature HIV-1 Protease, J. Mol. Biol. 428 (2016) 2780–2792.
[130] N.V. Nucci, B. Fuglestad, E.A. Athanasoula, A.J. Wand, Role of cavities and hydration in the pressure unfolding of T4 lysozyme, Proc. Natl. Acad. Sci. U.S.A. 111 (2014) 13846–13851.
[131] A. Maeno, D. Sindhikara, F. Hirata, R. Otten, F.W. Dahlquist, S. Yokoyama, K. Akasaka, F.A.A. Mulder, R. Kitahara, Cavity as a source of conformational fluctuation and high-energy state: high-pressure NMR study of a cavity-enlarged mutant of T4 lysozyme, Biophys. J. 108 (2015) 133–145.
[132] M.J. Fossat, T.P. Dao, K. Jenkins, M. Dellarole, Y.S. Yang, S.A. McCallum, A.E. Garcia, D. Barrick, C. Roumestand, C. Royer, High-resolution mapping of a repeat protein folding free energy landscape, Biophys. J . 111 (2016) 2368–2376.
[133] G.A. de Oliveira, J.L. Silva, A hypothesis to reconcile the physical and chemical unfolding of proteins, Proc. Natl. Acad. Sci. U.S.A. 112 (2015) E2775–E2784.
[134] M. Sadqi, D. Fushman, V. Muñoz, Atom-by-atom analysis of global downhill protein folding, Nature 442 (2006) 317–321.
[135] N. Naganathan, V. Munoz, Determining denaturation midpoints in multiprobe equilibrium protein folding experiments, Biochemistry 47 (2008) 6752–6761.
[136] Y. Bai, J.S. Milne, L. Mayne, S.W. Englander, Protein stability parameters measured by hydrogen exchange, Proteins 20 (1994) 4–14.
[137] Y. Bai, J.S. Milne, L. Mayne, S.W. Englander, Primary structure effects on peptide group hydrogen exchange, Proteins 17 (1993) 75–86.
[138] E.J. Fuentes, A.J. Wand, Local stability and dynamics of apocytochrome b_{562} examined by the dependence of hydrogen exchange on hydrostatic pressure, Biochemistry 37 (1998) 9877–9883.
[139] J. Roche, M. Dellarole, J.A. Caro, D.R. Norberto, A.E. Garcia, B. Garcia-Moreno, C. Roumestand, C.A. Royer, Effect of internal cavities on folding rates and routes revealed by real-time pressure-jump NMR spectroscopy, J. Am. Chem. Soc. 135 (2013) 14610–14618.
[140] Y. Zhang, S. Kitazawa, I. Peran, N. Stenzoski, S.A. McCallum, D.P. Raleigh, C.A. Royer, High pressure ZZ-exchange NMR reveals key features of protein folding transition states, J. Am. Chem. Soc. 138 (2016) 15260–15266.
[141] G.J.A. Vidugiris, J.L. Markley, C.A. Royer, Evidence for a molten globule-like transition state in protein folding from determination of activation volumes, Biochemistry 34 (1995) 4909–4912.
[142] C.A. Royer, The nature of the transition state ensemble and the mechanisms of protein folding: a review, Arch. Biochem. Biophys. 469 (2008) 34–45.
[143] L. Frydman, T. Scherf, A. Lupulescu, The acquisition of multidimensional NMR spectra within a single scan, Proc. Natl. Acad. Sci. U.S.A. 99 (2002) 15858–15862.
[144] M. Gal, P. Schanda, B. Brutscher, L. Frydman, UtraSOFAST HMQC NMR and repetitive acquisition of 2D protein spectra at Hz rates, J. Am. Chem. Soc. 129 (2007) 1372–1377.
[145] G.T. Montelione, G. Wagner, 2D chemical exchange NMR spectroscopy by proton-detected heteronuclear correlation, J. Am. Chem. Soc. 111 (1989) 3096–3098.
[146] N.A. Farrow, O.W. Zhang, J.D. Forman-Kay, L.E. Kay, A heteronuclear correlation experiment for simultaneous determination of ^{15}N longitudinal decay and chemical exchange rates of systems in slow equilibrium, J. Biomol. NMR 4 (1994) 727–734.

[147] N.A. Farrow, O.W. Zhang, J.D. Forman-Kay, L.E. Kay, Characterization of the backbone dynamics of folded and denatured states of an SH3 domain, Biochemistry 36 (1997) 2390–2402.
[148] V.N. Uversky, Natively unfolded proteins: a point where biology waits for physics, Protein Sci. 11 (2002) 739–756.
[149] A.K. Dunker, C.J. Brown, J.D. Lawson, L.M. Iakoucheva, Z. Obradovic, Intrinsic disorder and protein function, Biochemistry 41 (2002) 6573–6582.
[150] P. Tompa, Intrinsically unstructured proteins, Trends Biochem. Sci. 27 (2002) 527–533.
[151] A.L. Fink, Natively unfolded proteins, Curr. Opin. Struct. Biol. 15 (2005) 35–41.
[152] H.J. Dyson, P.E. Wright, Unfolded proteins and protein folding studied by NMR, Chem. Rev. 104 (2004) 3607–3622.
[153] N. Tjandra, A. Bax, Direct measurement of distances and angles in biomolecules by NMR in a dilute liquid crystalline medium, Science 278 (1997) 1111–1114.
[154] J.H. Prestegard, H.M. al-Hashimi, J.R. Tolman, NMR structures of biomolecules using field oriented media and residual dipolar couplings, Q. Rev. Biophys. 33 (2000) 371–424.
[155] M. Blackledge, Recent progress in the study of biomolecular structure and dynamics in solution from residual dipolar couplings, Prog. Nucl. Magn. Reson. Spectrosc. 46 (2005) 23–61.
[156] S. Meier, M. Blackledge, S. Grzesiek, Conformational distributions of unfolded polypeptides from novel NMR techniques, J. Chem. Phys. 128 (2008) 052204.
[157] D. Shortle, M.S. Ackerman, Persistence of native-like topology in a denatured protein in 8 M urea, Science 293 (2001) 487–489.
[158] A.T. Alexandrescu, R.A. Kammerer, Structure and disorder in the ribonuclease S-peptide probed by NMR residual dipolar couplings, Protein Sci. 12 (2003) 2132–2140.
[159] R. Mohana-Borges, N.K. Goto, G.J.A. Kroon, H.J. Dyson, P.E. Wright, Structural characterization of unfolded states of apomyoglobin using residual dipolar couplings, J. Mol. Biol. 340 (2004) 1131–1142.
[160] W. Fieber, S. Kristjansdottir, F.M. Poulsen, Short-range, long-range and transition state interactions in the denatured state of ACBP from residual dipolar couplings, J. Mol. Biol. 339 (2004) 1191–1199.
[161] S. Meier, S. Güthe, T. Kiefhaber, S. Grzesiek, Foldon, the natural trimerization domain of T4 fibritin, dissociates into a monomeric A-state form containing a stable beta-hairpin: atomic details of trimer dissociation and local beta-hairpin stability from residual dipolar couplings, J. Mol. Biol. 344 (2004) 1051–1069.
[162] S. Ohnishi, A.L. Lee, M.H. Edgell, D. Shortle, Direct demonstration of structural similarity between native and denatured eglin C, Biochemistry 43 (2004) 4064–4070.
[163] K. Ding, J.M. Louis, A.M. Gronenborn, Insights into conformation and dynamics of protein GB1 during folding and unfolding by NMR, J. Mol. Biol. 335 (2004) 1299–1307.
[164] C.O. Sallum, D.M. Martel, R.S. Fournier, W.M. Matousek, A.T. Alexandrescu, Sensitivity of NMR residual dipolar couplings to perturbations in folded and denatured staphylococcal nuclease, Biochemistry 44 (2005) 6392–6403.
[165] G. Nodet, L. Salmon, V. Ozenne, S. Meier, M.R. Jensen, M. Blackledge, Quantitative description of backbone conformational sampling of unfolded proteins at amino acid resolution from NMR residual dipolar couplings, J. Am. Chem. Soc. 131 (2009) 17908–17918.
[166] M.R. Jensen, P. Markwick, C. Griesinger, M. Zweckstetter, S. Meier, S. Grzesiek, P. Bernado, M. Blackledge, Quantitative determination of the conformational properties of partially folded and intrinsically disordered proteins using NMR dipolar couplings, Structure 17 (2009) 1169–1185.
[167] E. Brunner, M.R. Arnold, W. Kremer, H.R. Kalbitzer, Pressure-stability of phospholipid bicelles: measurement of residual dipolar couplings under extreme conditions, J. Biomol. NMR 21 (2001) 173–176.
[168] Y. Fu, A.J. Wand, Partial alignment and measurement of residual dipolar couplings of proteins under high hydrostatic pressure, J. Biomol. NMR 56 (2013) 353–357.
[169] N. Sibille, M. Dellarole, C. Royer, C. Roumestand, Measuring residual dipolar couplings at high hydrostatic pressure: robustness of alignment media to high pressure, J. Biomol. NMR 58 (2014) 9–16.
[170] J. Roche, J.M. Louis, A. Bax, R.B. Best, Pressure-induced structural transition of mature HIV-1 protease from a combined NMR/MD simulation approach, Proteins 83 (2015) 2117–2123.
[171] I.C. Felli, B. Brutscher, Recent advances in solution NMR: fast methods and heteronuclear direct detection, Chem. Phys Chem. 10 (2009) 1356–1368.
[172] D. Sahu, M. Bastidas, S.A. Showalter, Generating NMR chemical shift assignments of intrinsically disordered proteins using carbon-detected NMR methods, Anal. Biochem. 449 (2014) 17–25.